Eur. Phys. J. C (2023) 83:1163
https://doi.org/10.1140/epjc/s10052-023-12317-w

THE EUROPEAN PHYSICAL JOURNAL C

Regular Article - Theoretical Physics

The nonleptonic decays of *b*-flavored mesons to *S*-wave charmonium and charm meson states

Kalpalata Dash[1,a], **P. C. Dash**[1], **R. N. Panda**[1], **Lopamudra Nayak**[2,b], **Susmita Kar**[3], **N. Barik**[4]

[1] Department of Physics, Siksha 'O' Anusandhan Deemed to be University, Bhubaneswar 751030, India
[2] National Institute of Science Education and Research (NISER), Bhubaneswar 752050, India
[3] Department of Physics, Maharaja Sriram Chandra Bhanja Deo University, Baripada 757003, India
[4] Department of Physics, Utkal University, Bhubaneswar 751004, India

Received: 31 March 2023 / Accepted: 4 December 2023 / Published online: 20 December 2023

Abstract The detection of radially excited charmonium and charm meson states, and measurement of heavy meson decays, particularly $B_c^+ \to J/\psi D_s^+$ and $B_c^+ \to J/\psi D_s^{*+}$, by the LHCb and ATLAS Collaborations, have aroused a lot of theoretical interest in the nonleptonic decays of *b*-flavored mesons. In this paper, we study the exclusive two-body nonleptonic $\bar{B}^0$, $\bar{B}_s^0$, B^- and B_c^--meson decays to two vector meson $(V_1(nS)V_2)$ states. Assuming the factorization hypothesis, we calculate the weak-decay form factors from the overlapping integrals of meson wave functions, in the framework of the relativistic independent quark (RIQ) model. We find a few dominant decay modes: $B^- \to D^{*0}\rho^-$, $\bar{B}^0 \to D^{*+}\rho^-$, $\bar{B}_s^0 \to D_s^{*+}\rho^-$, $B^- \to J/\psi K^{*-}$ and $B_c^- \to J/\psi D_s^{*-}$ with predicted branching fractions of 1.52, 1.40, 1.16, 0.46 and 0.27 (in %), which are experimentally accessible. The predicted branching fractions for corresponding decay modes to excited $(2S)$ states, obtained in $\mathcal{O}(10^{-3} - 10^{-4})$ lie within the detection accuracy of the current experiments at LHCb and Tevatron. Our predicted CP-odd fractions $(R_\perp)$ for color-favored B_c-decays to two charmful states $(D^* D_{(s)}^*)$ are found significant as compared to similar decay modes of other *b*-flavored mesons.

1 Introduction

Ever since the discovery of excited charmonium states: $\psi(2S)$ at SLAC [1] through a Second Narrow Resonance in e^+e^- Annihilation and $\eta_c(2S)$ by Belle Collaboration via decay channels $B^\pm \to K^\pm \eta_c(2S)$ and $\eta_c(2S) \to K_S^0 K^\pm \pi^\mp$ [2], many new excited heavy meson and heavy-light meson states have also been discovered, especially the radially excited states. In the heavy-light meson sector, some $2S$-state candidates have also been discovered. Looking at the measurement parameters like mass and spin-parity, excited states discovered by the Belle, LHCb and Delphi Collaborations in the charm meson sector may be identified as $2S$-state candidates even though the assignment of the newly discovered meson states as radially excited states are yet to be commonly accepted. The $D_{s1}^*(2710)^\pm$ discovered by Belle [3] may be considered theoretically to be $D_S^*(2S)^\pm$ [4]. The $D(2550)^0$ discovered by LHCb [5] has the mass close to the theoretical prediction of $D(2S)^0$ [6]. An unnatural state of $D_J(2580)^0$ [7] discovered by LHCb may also be candidate of $D(2S)^0$ and $D^*(2640)^\pm$ discovered by Delphi Collaboration [8] is found to have mass consistent with the predictions of $D^*(2S)^\pm$ [6]. The recent discovery of $D_1^*(2600)$ state by LHCb [9] may be identified as $D^*(2S)^0$ state. The current RUN-II at Tevatron, RUN-III at CERN LHC, and the e^+e^- collider activities at Belle-II are all designed to boost the measurement scenario in heavy flavor physics. Specially designed detectors at BTeV and LHCb, dedicated to enhancing the event accumulation rates, are expected to yield high statistics *b*-flavored (B, B_s) events and the B_c-events, in particular, at the rate $\sim 10^{10}$ events per annum; providing a fascinating area of research in B-physics. The measurement of B, B_s-meson decays by Belle, BaBar and LHCb Collaborations [10–12] and recent measurement of B_c-meson decays: $B_c \to J/\psi D_s$ and $B_c \to J/\psi D_s^*$, performed by LHCb [13] and ATLAS [14] Collaborations have aroused a great deal of theoretical interest in nonleptonic decays of heavy-flavored mesons. The study of nonleptonic decays of heavy mesons is important as it helps in probing the interplay of QCD and electroweak interactions, determining the Cabibbo–Kobayashi–Maskawa

[a] e-mail: kalpalatadash982@gmail.com (corresponding author)
[b] e-mail: lopalmn95@gmail.com

(CKM) matrix elements, testing predictions of the Standard Model (SM), and exploring new physics beyond SM.

The nonleptonic decays of b-flavored mesons have been widely studied in different theoretical and phenomenological model approaches (see the classified bibliography of Ref. [15]). Most of these earlier studies refer to the b-flavored (B, B_s, B_c)-meson decays to ground states of charmonium and charm mesons. A number of theoretical attempts have also been made in this sector, yielding predictions on decay modes to radially excited states. A few noteworthy among them include studies based on the non-relativistic potential model (NRPM) using the Bathe-Salpeter equation [16,17], relativistic constituent quark model (RCQM) based on the Bathe-Salpeter formalism [18], improved Bathe–Salpeter (IBS) approach [19,20], relativistic quark model (RQM) [21–24], ISGW2 quark model [25], covariant confined quark model (CCQM) [26], relativistic quark model (RQM) using quasi-potential approach [27], QCD relativistic potential model (QCDRPM) [28], QCD factorization [29], perturbative QCD (pQCD) [30], covariant light-front quark model (CLFQM) [31], light-cone sum rule (LCSR) [32] and the heavy quark sum rules (HQS) [33] etc. The recent predictions of branching fraction for $B_c \to J/\psi D_s^*(2S) \simeq 1.75\times10^{-2}$, $B_c \to \psi(2S)D_s^* \simeq 2.72\times10^{-3}$ based on improved Bathe–Salpeter approach [19,20], $B_s \to D_s^*(2S)D_s^* \simeq 1.7\times10^{-3}$ in RQM [27], $B_c^- \to \psi(2S)\rho^- \simeq 1.1\times10^{-3}$, $B_c \to \psi(2S)D_s^* \simeq 1.2\times10^{-3}$ in ISGW2 quark model [25], $B_c^+ \to D^{*+}\bar{D}^{*0} \simeq 5.14\times10^{-3}$ in QCDRPM [28] etc. are accessible in the LHCb experiment. The branching fractions for decay modes: $B_c^- \to \psi(2S)\rho^-$ [17], $B_s \to D_s^*\rho^-$ and $B_c^- \to \psi(3S)\rho^-$ [19], etc. predicted in the range $\sim 10^{-4}$, lie within the detection accuracy of the current experiments and can be measured in near future.

The analysis of nonleptonic decays is notoriously nontrivial as it is strongly influenced by confining color forces and it involves matrix elements of local four-quark operators in the non-perturbative QCD approach, the mechanism of which is not yet clear in the SM framework. Ignoring the weak annihilation contribution, the transition amplitudes can be conveniently described in the so-called naive factorization approximation [18,21–24,28,34–56], which works reasonably well in the nonleptonic b-flavored meson decays, where the quark-gluon sea is suppressed in the heavy quarkonium [48–51]. In this approach, the transition matrix element of local four-quark operators is factorized into two single current matrix elements. One of the factorized amplitudes, in which the decaying parent meson is connected to one final meson state, can be covariantly expanded in terms of Lorentz invariant weak form factors as in the case of semileptonic decays. The other factorized amplitude, where the vacuum is connected to the second final meson state, can be parametrized in terms of meson decay constants that describe the leptonic decays. The description of the nonleptonic decay process is thus reduced to the calculation of weak decay form factors in the framework of a suitable phenomenological model.

Bjorken's intuitive argument on color transparency in his pioneering work [52], theoretical development based on the QCD approach in the $\frac{1}{N_c}$ limit [53] and the heavy quark effective theory (HQET) [54], etc. justify the naive factorization approximation, where strong-interaction effects such as the final-state interaction, rescattering of the final state hadrons and the renormalization-point dependence of amplitudes are shown to be marginal [57]. Discovery of excited charmonium and charm meson states and prediction of b-flavored meson decays to the ground and radially excited states by different theoretical approaches, inspired our group to predict energetic nonleptonic B and $B_c \to PP, PV, VP$ decays [34,35] as well as their decays to two vector meson (VV) ground states [36,37], within the framework of our relativistic independent quark (RIQ) model. Here $P(V)$ refers to a pseudoscalar (vector) meson state. The nonleptonic B_c-decays to an S-wave charmonium and a light or charm meson state [56] have also been predicted by our group in good comparison with the experiment and other SM predictions.

Note here that the approach based on naive factorization approximation may be justified in the analysis of energetic nonleptonic decays of $B_F \to PP, PV$ type, with the quark flavor $F \to d, u, s, c$; where the strong interaction effects such as the final state interaction, rescattering of final state meson as well as the renormalization point dependence of factorized amplitude have been shown to be marginal [58]. Such an approach, however, may not hold up well in the description of $B_F \to V_1(nS)V_2$ decays, where both the final state mesons being heavy, are expected to be in the region close to zero recoil point. Here also both the longitudinal and transverse polarization components contribute to decay amplitude which can be measured experimentally. From the naive counting rules, the longitudinal polarization fraction in this sector is expected to dominate over transverse components which can be checked as well. The nonleptonic B_F-decays to two charmful vector meson states are of special interest. They provide ideal modes to check the factorization hypothesis as the phenomenon of color transparency applicable to the light energetic hadron is not valid in these cases.

In this paper we would like to extend the applicability of our RIQ model to study, within factorization approximation, the nonleptonic $B_F \to V_1(nS)V_2$ decays to S-wave charmonium and charmed vector meson states (nS) along with a light or a heavy-light meson state, where $n = 1, 2, 3$. We ignore the decay channels involving higher $(4S)$ charmonium and charm meson states since their properties are still not understood well. We adopt here the general formalism used in Ref. [56]. In the present study we consider the contribution of the current-current operators [59] only in calculating the tree-level diagram, expected to be dominant in $B_F \to V_1(nS)V_2$

decays. The contribution of the penguin diagram may be significant in the evaluation of CP-violation and search for new physics beyond SM, but its contribution to these decay amplitudes is considered less significant. In fact, the QCD and electroweak penguin operators' contribution have been shown [60–63] negligible compared to the contribution of current-current operators in these decays due to serious suppression of CKM matrix elements. The Wilson's coefficients of penguin operators being very small, their contribution to decay amplitude is only relevant in rare decays, where the tree-level contribution is either strongly CKM-suppressed as in $\bar{B} \to \bar{K}^*\pi$ or matrix elements of current-current operators do not contribute at all as in the case of rare decays: $\bar{B} \to \bar{K}^*\gamma$ and $\bar{B}^0 \to \bar{K}^0\phi$ [59].

The rest of the paper is organized as follows. In the following section, we present a general remark on the factorization approximation and discussed the factorized amplitudes of the nonleptonic decay. In Sect. 3, we obtain the model expressions for invariant weak-decay form factors and the factorized transition amplitudes. Section 4 is devoted to the numerical results and discussion and Sect. 5 encompasses our brief summary and conclusion. A brief review of the model conventions, wave-packet representation of the meson state and momentum probability amplitudes of the constituent quarks inside the meson bound-state are given in the Appendix.

2 Factorization approximation and nonleptonic transition amplitude

The transition amplitude for two-body nonleptonic transition: $B_F \to V_1(nS)V_2$ can be written as

$$A(B_F \to V_1(nS)V_2) = \langle V_1(nS)V_2|\mathscr{H}|B_F\rangle = \frac{G_F}{\sqrt{2}}\sum_i \lambda_i C_i(\mu)\langle\mathscr{O}\rangle_i, \quad (1)$$

where G_F is the Fermi coupling constant, λ_i the CKM factor, C_i is the Wilson coefficients and $\langle\mathscr{O}\rangle_i$ is the matrix element of local four-quark operators. In the factorization approximation, the matrix element of the local four-quark operator is factorized into two single-particle matrix elements of quark current as

$$\langle V_1(nS)V_2|\mathscr{H}|B_F\rangle_i = \langle V_2|J^\mu|0\rangle\langle V_1(nS)|J_\mu|B_F\rangle + (V_1(nS) \leftrightarrow V_2), \quad (2)$$

where $J_\mu \equiv V_\mu - A_\mu$ is the vector-axial vector current.

The difficulty inherent in such an approach is that Wilson's coefficients $C_i(\mu)$, which include the short distance QCD effect between $\mu = m_N$ and $\mu = m_b$ are μ scale and renormalization scheme dependent, whereas $\langle\mathscr{O}\rangle_i$ are μ scale and renormalization scheme independent. As a result, physical amplitude depends on the μ scale. However, in the naive factorization approach, the long-distance effects are disentangled from the short-distance effect assuming that the matrix element $\langle\mathscr{O}\rangle$ at the μ scale contains nonfactorizable contributions. This results in the cancellation of the μ dependence and scheme dependence of $C_i(\mu)$.

We neglect here the so-called W exchange and annihilation diagram, since in the limit $M_W \to \infty$ they are connected by Fiertz transformation and doubly suppressed by a kinematic factor of order $(\frac{m_i^2}{M_W^2})$ [53]. We also discard the color octet current which emerges after the Fiertz transformation of color singlet operators. Clearly, these currents violate factorization since they cannot provide transitions to vacuum states. Taking into account the Fiertz reordered contribution, the relevant coefficients are not $C_1(\mu)$ and $C_2(\mu)$ but the combination

$$a_{1,2}(\mu) = c_{1,2}(\mu) + \frac{1}{N_c}c_{2,1}(\mu). \quad (3)$$

The factorization approximation, in general, works well in the description of two-body nonleptonic decays of heavy mesons in the limit of a large number of colors. Assuming a large N_c limit to fix the QCD coefficients $a_1 \approx c_1$ and $a_2 \approx c_2$ at $\mu \approx m_b^2$, nonleptonic decays of heavy mesons have been analyzed in Refs. [16,25,64–68].

The hadronic matrix element of the weak current J_μ are covariantly expanded in terms of weak form factors as

$$\langle V_1(\mathbf{k})|A_\mu|B_F(\mathbf{p})\rangle = f(q^2)\epsilon_\mu^* + a_+(q^2)(\epsilon^*.p)(p+k)_\mu + a_-(q^2)(\epsilon^*.p)(p-k)_\mu, \quad (4)$$

$$\langle V_1(\mathbf{k})|V_\mu|B_F(\mathbf{p})\rangle = ig(q^2)\epsilon_{\mu\nu\rho\sigma}\epsilon^{*\nu}(p+k)^\rho(p-k)^\sigma, \quad (5)$$

where ϵ^* is the polarization of the vector meson V_1. p and k represent the four-momentum of the parent meson B_F and daughter meson V_1, respectively. With the four-momentum transfer $q = p - k \equiv (E, 0, 0, |\mathbf{q}|)$ and mass m_{V_1}, the polarization of the daughter meson V_1 is taken in the form

$$\epsilon_\mu^\pm \equiv \frac{1}{\sqrt{2}}(0, \mp 1, -i, 0),\ \epsilon_\mu^L \equiv \frac{1}{m_{V_1}}(|\mathbf{q}|, 0, 0, E). \quad (6)$$

The matrix element of the current J^μ between vacuum and vector-meson V_2 in the final state can be parametrized in terms of meson decay constant f_{V_2} as

$$\langle V_2|J^\mu|0\rangle = \epsilon_{V_2}^{*\mu} f_{V_2} m_{V_2}. \quad (7)$$

In the factorization approach, the nonleptonic transition amplitude can be calculated from one of the three possible tree-level diagrams shown in Fig. 1. The color-favored transitions, shown in quark level diagram in Fig. 1a, represent "class I" transitions which are characterized by external emission of W-boson. In these transitions, the factorized amplitudes coupled to the QCD factor a_1 only give the nonvanishing contribution. On the other hand, color-suppressed

transitions shown in the diagram in Fig. 1b representing "class II" transitions are characterized by internal W emission. In such transitions, the nonvanishing contribution to the decay rate comes from factorized amplitude proportional to the QCD factor a_2. Figure 1c, however, represents "class III" transitions which are due to both color-favored and color-suppressed diagrams. In such decays, the factorized amplitudes corresponding to a_1 and a_2 contribute coherently to give the transition amplitude.

For the color-favored general type tree-level transition $B_F \to V_1(nS)V_2$ pertaining to "class I" transitions, the decay rate can be written as [36,37,47]

$$\Gamma = \frac{{G_F}^2}{16\pi} a_1^2(\mu) |V_{bq'} V_{q_i\bar{q}_j}|^2 \frac{|\mathbf{k}|}{M^2} |\mathscr{A}|^2, \tag{8}$$

where M and $\mathbf{k}$ represent the parent-meson mass and three-momentum of the recoiled daughter meson V_1, respectively, in the parent-meson rest frame. $|\mathscr{A}|^2$ is the sum of the polarized amplitude squared with $\mathscr{A}_j \equiv \langle V_2|J^\mu|0\rangle\langle V_1|J_\mu|B_F\rangle$, such that

$$|\mathscr{A}|^2 = \sum_j |\mathscr{A}_j|^2. \tag{9}$$

We use the notation $j = \pm, \mp$ or ll, where the first and second labels denote the helicity of the V_1 and V_2 meson, respectively. From the polarized amplitudes expressed in terms of the weak form factors f, g and a_+ and the decay constant f_{V_2} shown in Eqs. (4)–(7), it is straightforward to find expressions for the positive, negative, and longitudinal polarizations, respectively, of the daughter meson V_1 as

$$\begin{aligned}
\mathscr{A}_\pm &= -f_{V_2} m_{V_2} \{f(q^2) + 2g(q^2)|\mathbf{k}|M\},\\
\mathscr{A}_\mp &= -f_{V_2} m_{V_2} \{f(q^2) - 2g(q^2)|\mathbf{k}|M\},\\
\mathscr{A}_{ll} &= \frac{f_{V_2}}{m_{V_1}} \Bigg[f(q^2) \Big\{ |\mathbf{k}|^2 + \frac{1}{4M^2}(M^2 + m_{V_1}^2 - m_{V_2}^2)\\
&\quad \times (M^2 + m_{V_2}^2 - m_{V_1}^2) \Big\} + 2a_+(q^2)|\mathbf{k}|^2 M^2 \Bigg],
\end{aligned} \tag{10}$$

where

$$|\mathbf{k}| = \left[\left(\frac{M^2 + m_{V_1}^2 - m_{V_2}^2}{2M} \right)^2 - m_{V_1}^2 \right]^{1/2}. \tag{11}$$

The decay widths for $B_F \to V_1(nS)V_2$ decays can be predicted from Eq. (8) using the expressions in Eqs. (9–11) for the polarized amplitudes in terms of the weak form factors derivable in the framework of the RIQ model.

3 Transition amplitude and weak form factors

As discussed in the preceding section, the nonleptonic transition amplitude for the process $B_F \to V_1(nS)V_2$ can be calculated from the tree-level diagram shown in Fig. 1. The class-I type decay modes, depicted in Fig. 1a, are induced by the b-quark transition to the daughter quark q' with the emission of W-boson. The daughter quark q' and the antiquark $\bar{q}$ of the decaying parent meson state $|B_F(\mathbf{p}, S_{B_F})\rangle$ hadronize to form a vector meson state $|V_1(\mathbf{k}, S_{V_1})\rangle$. The externally emitted W-boson first decays to a quark-antiquark pair ($q_i\,\bar{q}_j$), which subsequently hadronizes to other vector meson state $|V_2(\mathbf{q}, S_{V_2})\rangle$.

The decay process, in fact, occurs physically in the momentum eigenstate of participating mesons. Therefore, a field-theoretic description of a decay process demands meson-bound states to be represented by appropriate momentum wave packets reflecting momentum and spin distribution between the quark constituents in the meson core. A brief discussion of the wave-packet representation of meson bound state in the RIQ model is given in the Appendix. Using the wave-packet representation (A.9–A.11) of participating meson states, the residual dynamics responsible for the decay process can, therefore, be described at the constituent level by the otherwise unbound quark and antiquark using the usual Feynman technique. The constituent-level S-matrix element $S_{fi}^{b\to q' q_i\bar{q}_j}$ obtained from the appropriate Feynman diagram when operated upon by the bag-like operator $\hat{\Lambda}(\mathbf{p}, S_{B_F})$ in the wave packet representation can give rise to the mesonic-level S-matrix element in the form

$$S_{fi}^{B_F\to V_1(nS)V_2} \to \hat{\Lambda}(\mathbf{p}, S_{B_F})\, S_{fi}^{b\to q' q_i\bar{q}_j}. \tag{12}$$

Using the wave packet representation of the parent and daughter meson state, $|B_F(\mathbf{p}, S_{B_F})\rangle$ and $|V_1(\mathbf{k}, S_{V_1})\rangle$, respectively, we calculate the Feynman diagram Fig. 1a and obtain the S-matrix element in the parent meson rest frame in the general form:

$$\begin{aligned}
S_{fi} &= (2\pi)^4\, \delta^{(4)}(M - q - k)\, (-i\mathscr{M}_{fi}) \frac{1}{\sqrt{V2M}}\\
&\quad \prod_f \frac{1}{\sqrt{V2E_f}},
\end{aligned} \tag{13}$$

where the invariant transition amplitude $\mathscr{M}_{fi}$ is obtained in the form:

$$\mathscr{M}_{fi} = \frac{G_F}{\sqrt{2}} V_{bq'} V_{q_i\bar{q}_j} a_1 \mathscr{A}, \tag{14}$$

with $\mathscr{A} = h^\mu H_\mu$, $h^\mu = \epsilon_{V_2}^{*\mu}(\mathbf{q}, \lambda_2) f_{V_2} m_{V_2}$ and

$$\begin{aligned}
H_\mu &= \frac{1}{\sqrt{N_{B_F}(0) N_{V_1}(\mathbf{k})}} \int d^3\mathbf{p}_b\\
&\quad \times \frac{\mathscr{G}_{B_F}(\mathbf{p}_b, -\mathbf{p}_b)\, \mathscr{G}_{V_1}(\mathbf{p}_b + \mathbf{k}, -\mathbf{p}_b)}{\sqrt{E_b(\mathbf{p}_b) E_{q'}(\mathbf{p}_b + \mathbf{k})}}\\
&\quad \times \sqrt{[E_b(\mathbf{p}_b) + E_{\bar{q}}(-\mathbf{p}_b)][E_{q'}(\mathbf{p}_b + \mathbf{k}) + E_{\bar{q}}(-\mathbf{p}_b)]}\\
&\quad \times \langle S_{V_1}|J_\mu(0)|S_{B_F}\rangle.
\end{aligned} \tag{15}$$

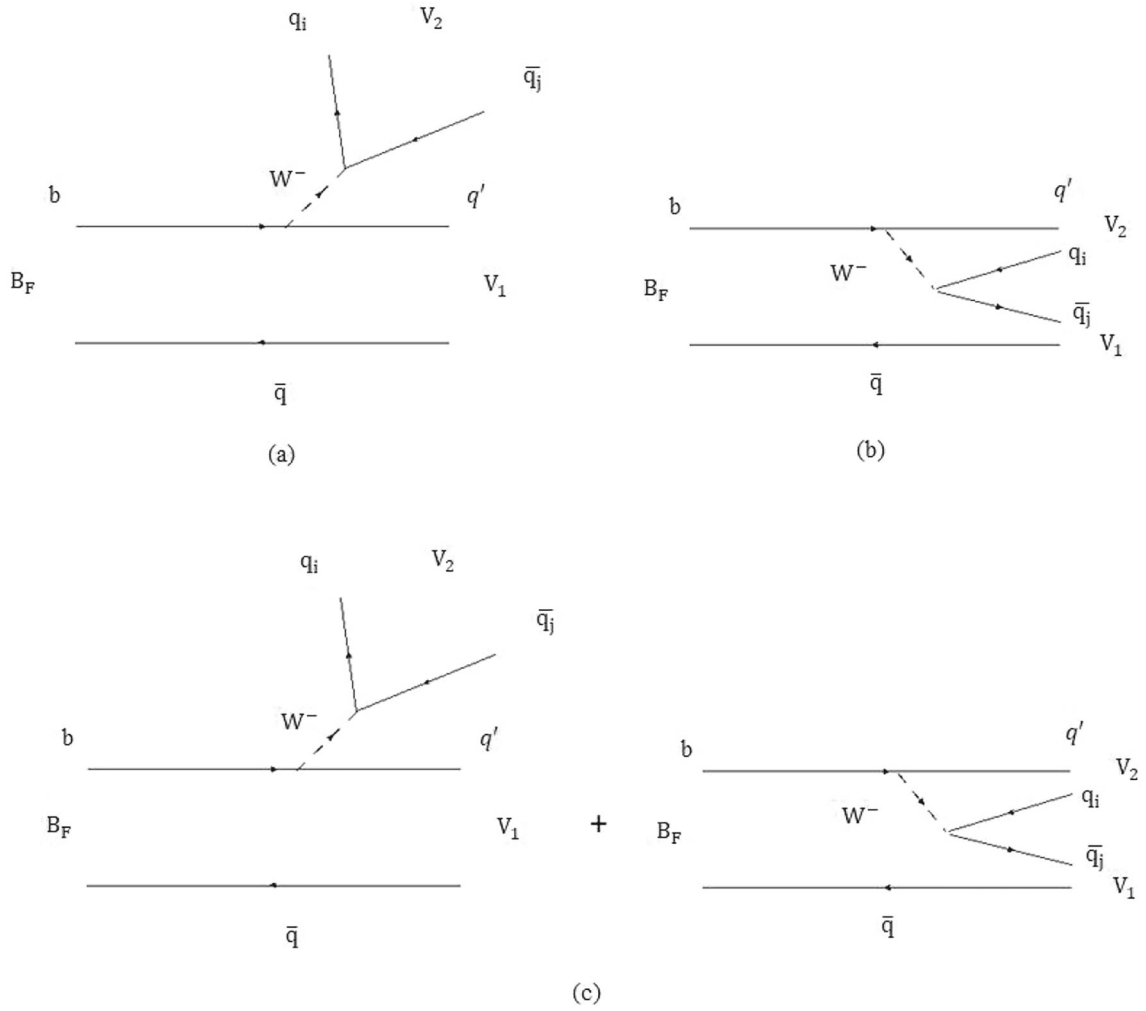

Fig. 1 Quark-level diagram of the nonleptonic meson decays: $B_F \to V_1(nS)V_2$

The terms $E_b(\mathbf{p}_b)$ and $E_{q'}(\mathbf{p}_b + \mathbf{k})$ in (15) stand for the energy of the non-spectator quark of the parent and daughter meson, $\mathbf{p}_b$ and $\mathbf{k}$ represent three momentum of the non-spectator constituent quark b and the daughter meson V_1, respectively and $q = p - k$ is the four-momentum transfer. Finally, $\langle S_V|J_\mu|S_{B_F}\rangle$ is the symbolical representation of the spin matrix elements of the effective vector-axial vector current; which can be written in the explicit form:

$$\begin{aligned}\langle S_{V_1}|J_\mu(0)|S_{B_F}\rangle &= \sum_{\lambda_b,\lambda_{q'},\lambda_{\bar{q}}} \zeta^{B_F}_{b\bar{q}}(\lambda_b,\lambda_{\bar{q}})\,\zeta^{V_1}_{q'\bar{q}}(\lambda_{q'},\lambda_{\bar{q}}) \\ &\times \bar{u}_{q'}(\mathbf{p}_b+\mathbf{k},\lambda_{q'})\,\gamma_\mu(1-\gamma_5)\,\gamma_\mu(1-\gamma_5) \\ &u_b(\mathbf{p}_b,\lambda_b)u_b(\mathbf{p}_b,\lambda_b) \qquad (16)\end{aligned}$$

Here, u_i stands for free Dirac spinor. $\zeta^{B_F}(\lambda_b,\lambda_{\bar{q}})$ and $\zeta^{V_1}(\lambda_{q'},\lambda_{\bar{q}})$ are the appropriate $SU(6)$ spin flavor coefficients corresponding to the parent and daughter meson, respectively.

It may be pointed out here that, in our description of the decay process, $B_F \to V_1(nS)V_2$ the three momentum conservation is ensured explicitly via $\delta^{(3)}(\mathbf{p}_b + \mathbf{p}_{\bar{q}} - \mathbf{p})$ and $\delta^{(3)}(\mathbf{p}_i + \mathbf{p}_j - \mathbf{k})$ in the participating meson states. However, energy conservation in such a scheme is not ensured so explicitly. This is in fact a typical problem in all potential model descriptions of mesons as bound states of valence quarks and antiquarks interacting via some instantaneous potential. This problem has been addressed in the previous analysis in this model in the context of radiative leptonic decays of heavy flavored meson B, B_c, D, D_s [69–71] and also in the QCD relativistic quark model [72,73], where the effective momentum distribution function $\mathscr{G}_{B_F}(\mathbf{p}_b,\mathbf{p}_{\bar{q}})$ that embodies bound-state characteristics of the meson, ensures energy conservation in an average sense satisfying $E_M = \langle B_F(\mathbf{p},S_{B_F})|[E_b(\mathbf{p}_b) + E_{\bar{q}}(\mathbf{p}_{\bar{q}})]|B_F(\mathbf{p},S_{B_F})\rangle$. In view of this, we take the energy conservation constraint $M = E_b(\mathbf{p}_b) + E_{\bar{q}}(-\mathbf{p}_b)$ in the parent meson rest frame. This along with the three momentum conservation via appro-

priate $\delta^{(3)}(\mathbf{p}_b + \mathbf{p}_{\bar{q}} - \mathbf{p})$ in the meson state ensures the required four-momentum conservation $\delta^{(4)}(p-k-q)$ at the mesonic level, which is pulled out of the quark-level integration to obtain the S-matrix element in the standard form (13). This has been discussed elaborately in earlier works [34–37,56].

Using usual spin algebra the spacelike and timelike components of the spin matrix elements $\langle S_{V_1}|J_\mu(0)|S_{B_F}(0)\rangle$ corresponding to vector and axial vector current are obtained in the form

$$\langle S_{V_1}(\mathbf{k},\hat{\epsilon}^*_{V_1})|V_0|S_{B_F}(0)\rangle = 0, \tag{17}$$

$$\langle S_{V_1}(\mathbf{k},\hat{\epsilon}^*_{V_1})|V_i|S_{B_F}(0)\rangle = \frac{i[E_b(\mathbf{p}_b)+m_b]}{\sqrt{[E_b(\mathbf{p}_b)+m_b][E_{q'}(\mathbf{p}_b+\mathbf{k})+m_{q'}]}}(\hat{\epsilon}^*_{V_1}\times\mathbf{k})_i, \tag{18}$$

$$\langle S_{V_1}(\mathbf{k},\hat{\epsilon}^*_{V_1})|A_i|S_{B_F}(0)\rangle = \frac{[E_b(\mathbf{p}_b)+m_b][E_{q'}(\mathbf{p}_b+\mathbf{k})+m_{q'}]-(\mathbf{p}_b^2/3)}{\sqrt{[E_b(\mathbf{p}_b)+m_b][E_{q'}(\mathbf{p}_b+\mathbf{k})+m_{q'}]}}(\hat{\epsilon}^*_{V_1})_i, \tag{19}$$

$$\langle S_{V_1}(\mathbf{k},\hat{\epsilon}^*_{V_1})|A_0|S_{B_F}(0)\rangle = \frac{[E_b(\mathbf{p}_b)+m_b]}{\sqrt{[E_b(\mathbf{p}_b)+m_b][E_{q'}(\mathbf{p}_b+\mathbf{k})+m_{q'}]}}(\hat{\epsilon}^*_{V_1}.\mathbf{k}). \tag{20}$$

Here, $E_b(\mathbf{p}_b)=\sqrt{\mathbf{p}_b^2+m_b^2}$ and $E_{q'}(\mathbf{p}_b+\mathbf{k})=\sqrt{(\mathbf{p}_b+\mathbf{k})^2+m_{q'}^2}$ are, respectively, the energy of the non-spectator quark b and daughter quark q'. The spacelike component of the hadronic matrix element H_μ obtained from Eq. (15) via Eqs. (18) and (19) are compared with the corresponding expressions from Eqs. (4) and (5), which lead to the model expressions of the weak form factors $g(q^2)$ and $f(q^2)$ in the form:

$$g(q^2) = -\frac{1}{2M}\int d\mathbf{p}_b\, \mathscr{Q}(\mathbf{p}_b)\,[E_b(\mathbf{p}_b)+m_b], \tag{21}$$

$$f(q^2) = -\int d\mathbf{p}_b \mathscr{R}(\mathbf{p}_b), \tag{22}$$

where

$$\mathscr{Q}(\mathbf{p}_b) = \frac{\mathscr{G}_{B_F}(\mathbf{p}_b,-\mathbf{p}_b)\mathscr{G}_{V_1}(\mathbf{p}_b+\mathbf{k},-\mathbf{p}_b)}{\sqrt{N_{B_F}(0)N_{V_1}(\mathbf{k})}} \times\frac{\sqrt{[E_b(\mathbf{p}_b)+E_{\bar{q}}(-\mathbf{p}_b))][E_{q'}(\mathbf{p}_b+\mathbf{k})+E_{\bar{q}}(-\mathbf{p}_b)]}}{\sqrt{E_b(\mathbf{p}_b)E_{q'}(\mathbf{p}_b)[E_b(\mathbf{p}_b)+m_b][E_{q'}(\mathbf{p}_{q'})+m_{q'}]}}, \tag{23}$$

$$\mathscr{R}(\mathbf{p}_b) = \mathscr{Q}(\mathbf{p}_b)\Big[(E_b(\mathbf{p}_b)+m_b)(E_{q'}(\mathbf{p}_{q'})+m_{q'}) - \frac{\mathbf{p}_b^2}{3}\Big]. \tag{24}$$

The timelike component of hadronic amplitude obtained from Eq. (15) via Eq. (20), when compared with the corresponding expression from Eq. (4) yields an expression of the form factor $a_+(q^2)$ in the form:

$$a_+(q^2) = \frac{1}{2M^2}\Big[E_{V_1}\int d\mathbf{p}_b\, \mathscr{Q}(\mathbf{p}_b)\,(E_b(\mathbf{p}_b)+m_b) - \int d\mathbf{p}_b\, \mathscr{R}(\mathbf{p}_b)\Big]. \tag{25}$$

Then it is straightforward to get the model expression for the polarized amplitude squared $|\mathscr{A}_j|^2$ using Eqs. (21–25). Summing over possible polarization states and integrating over the final-state particle momenta, the decay width $\Gamma(B_F \to V_1(nS)V_2)$ is obtained in the parent-meson rest frame from the generic expression

$$\Gamma(B_F \to V_1(nS)V_2) = \frac{1}{(2\pi)^2}\int \frac{d\mathbf{k}\,d\mathbf{q}}{2M2E_{V_1}2E_{V_2}} \times\delta^{(4)}(p-k-q)\times\sum|\mathscr{M}_{fi}|^2. \tag{26}$$

The two-body nonleptonic decay $(B_F \to V_1(nS)V_2)$, described so far in this section refers to the color-favored "class I" decays involving external emission of W-boson. Similarly, class II and III type $B_F \to V_1(nS)V_2$ decays can be calculated from the corresponding Feynman diagrams shown in Fig. 1b, c, respectively. The model expressions for relevant form factors and decay rates for such decays (class II and class III) can be obtained by suitable replacement of appropriate flavor degree of freedom, quark masses, quark binding energies, QCD factors a_1, a_2, and the meson decay constants.

4 Numerical results and discussion

In this section, we present our numerical results in comparison with other model predictions and the available experimental data. For numerical calculation, we use the model parameters (a, V_0), quark mass parameter (m_q) and quark binding energy parameter (E_q), which have been fixed from hadron spectroscopy by fitting the data of heavy and heavy-light flavored mesons in their ground state as [74–76]

$$\begin{aligned}(a, V_0) &= (0.017166\ GeV^3, -0.1375\ GeV),\\ (m_b, m_c) &= (4.77659, 1.49276)\ GeV,\\ (m_s, m_u = m_d) &= (0.31575, 0.07875)\ GeV,\\ (E_b, E_c) &= (4.76633, 1.57951)\ GeV,\\ (E_s, E_u = E_d) &= (0.591, 0.47125)\ GeV.\end{aligned} \tag{27}$$

In the description of the decay process involving radially excited meson states, the constituent quarks in the meson-bound states are expected to have higher binding energies compared to their ground-state binding energies. For this, we solve the cubic equation representing the binding energy condition (A.5) for respective constituent quarks $(c, s, u = d)$ in radially excited $2S$ and $3S$ states of the $(\bar{c}c)$, $(\bar{c}u)$, $(\bar{c}d)$ systems as

$$\begin{aligned}(E_c, E_s, E_u = E_d)_{2S} &= (1.97015, 1.07737, 0.96221)GeV,\\ (E_c, E_s, E_u = E_d)_{3S} &= (2.22478, 1.40043, 1.29359)GeV.\end{aligned} \tag{28}$$

Table 1 The masses and decay constants of mesons

Particle	Mass (MeV)	Decay constant (MeV)	
		Experiment	Our prediction
ρ^-	775.11 [87]	207 [87]	...
$K^{*\pm}$	891.67 [87]	202.5 [87]	...
$D^{*0}(1S)$	2006.8 [87]	...	197
$D^{*\pm}(1S)$	2010.2 [87]	...	197
$D_s^{*\pm}(1S)$	2112.2 [87]	...	236
$J/\psi(1S)$	3096.9 [87]	416 [88]	...
B_c^-	6274.47 [87]		
$\bar{B}^0$	5279.66 [87]		
$\bar{B}_s^0$	5366.92 [87]		
B^-	5279.34 [87]		
$D^{*\pm}(2S)$	2637 [8]		
$D^{*0}(2S)$	2681 [9]		
$D_s^{*\pm}(2S)$	2732 [89]		
$\psi(2S)$	3686.1 [87]	304 [88]	...
$D^{*0}(3S)$	3080 [19]		
$D^{*\pm}(3S)$	3110 [89]		
$D_s^{*\pm}(3S)$	3193 [89]		
$\psi(3S)$	4039.1 [87]	174 [88]	...

Using the input parameters (27, 28), wide-ranging hadronic phenomena, which include the radiative, weak radiative, rare radiative, leptonic, weak leptonic, radiative leptonic and semileptonic decays [69–71,76–86] have been described within the framework of RIQ model. Exclusive two body nonleptonic decays of B and B_c mesons to the charmonium, charm, strange and non-strange light meson states have also been described [34–37,56] in this model. For CKM parameters and the lifetime of decaying mesons, we take their respective central values from the Particle Data Group (2022) [87] as:

$$\begin{aligned}(V_{bc}, V_{bu}) &= (0.0408, 0.00382),\\ (V_{cs}, V_{cd}) &= (0.975, 0.221),\\ (V_{us}, V_{ud}) &= (0.2243, 0.97373),\end{aligned} \tag{29}$$

and

$$\begin{aligned}(\tau_{B_c^-}, \tau_{B^-}) &= (0.510, 1.638)\ ps,\\ (\tau_{\bar{B^0}}, \tau_{\bar{B_s^0}}) &= (1.519, 1.521)\ ps,\end{aligned} \tag{30}$$

respectively. For the mass and decay constant of the participating mesons, considered as phenomenological inputs in the numerical calculation, we take the central values of the available observed data from Refs. [8,9,87,88]. In the absence of observed data in the charm meson sector, we predict the D^* and D_s^* meson decay constants from Eq. (7). Accordingly, the updated meson masses and decay constants used in the present study are listed in Table 1.

It may be mentioned here that, in the prediction of nonleptonic decay, uncertainties mostly creep into the calculation through input parameters: potential parameter (a, V_0), quark mass parameter (m_q) and quark binding energy parameter (E_q), CKM parameters, meson decay constants and QCD coefficients (a_1, a_2) etc. As mentioned above, the potential parameters, quark mass and quark binding energy parameters (27, 28) have already been fixed at the static level application of the RIQ model by fitting the mass spectra of heavy and heavy-light mesons. In order to avoid uncertainty in our model predictions, we take the central values of the CKM parameter as well as the observed value of the decay constants. As such we do not have the liberty to use any free parameter in our calculation which could be fine-tuned from time to time to predict hadronic phenomena. In that sense, we perform almost a parameter-free calculation in our studies. As regards the QCD coefficients: (a_1, a_2), different sets of data for decays induced by the b-quark transition at the quark level, are used in the literature. For example, Colangelo and De Fazio, in Ref. [28] use QCD coefficients, Set 1: $(a_1^b, a_2^b) = (1.12, -0.26)$, as fixed in Refs. [90,91]. In most earlier calculations, the authors use a different set of QCD coefficients, Set 2: $(a_1^b, a_2^b) = (1.14, -0.2)$, fixed by Buras et al. [53] in the mid-1980s, whereas Dubnicka et al. [92] use a different set of numerical value, i.e., Set 3: $(a_1^b, a_2^b) = (0.93, -0.27)$. We use all three sets of the Wilson coefficients in our calculation.

Before using the above input parameters in our numerical analysis, it is pertinent to elaborate a bit on the energy conservation ansatz mentioned in Sect. 3. The present analysis based on the energy conservation constraints $M =$

Table 2 The rms values of quark momentum, expectation values of the energy of quark and antiquark, and the sum of the energy of quark and antiquark in the meson states

Meson state $\|X(0)\rangle$	$\sqrt{\langle\|\mathbf{p}_b^2\|\rangle}$ (GeV)	$\langle E_b(\mathbf{p}_b^2)\rangle$ (GeV)	$\langle E_{\bar{q}}(\|-\mathbf{p}_b^2\|)\rangle$ (GeV)	$\langle[E_b(\mathbf{p}_b^2)+E_{\bar{q}}(\|-\mathbf{p}_b^2\|)]\rangle$ (GeV)	Observed meson mass (GeV)
$\|B_u(0)\rangle$	0.51	4.799	0.480	5.279	5.27934
$\|B_c(0)\rangle$	0.66	4.657	1.629	6.286	6.27447
$\|D(0)\rangle$	0.4506	1.4418	0.4275	1.8693	1.86966
$\|D_s(0)\rangle$	0.4736	1.4165	0.5517	1.9682	1.96835

$E_b(\mathbf{p}_b) + E_{q'}(-\mathbf{p}_b)$ in the parent meson rest frame might lead to spurious kinematic singularities at the quark-level integration appearing in the decay amplitude. This problem has already been addressed in the QCD relativistic quark model approach [72,73] and later by our group in the study of radiative leptonic decays of heavy and heavy-light flavored meson sector [69–71], by assigning a running mass m_b to the non-spectator quark that satisfies the relation:

$$m_b^2(|\mathbf{p}_b|) = M^2 + m_{\bar{q}}^2 - 2M\sqrt{|\mathbf{p}_b|^2 + m_{\bar{q}}^2},$$

as an outcome of the energy conservation ansatz, while retaining definite mass $m_{\bar{q}}$ of the spectator quark $\bar{q}$. This leads to an upper bound on the quark momentum $|\mathbf{p}_b| < \frac{M^2-m_{\bar{q}}^2}{2M}$ in order to retain $m_b^2(|\mathbf{p}_b|)$ positive definite. The upper limit $|\mathbf{p}_b|_{max}$ would have no other bearing to seriously affect the calculation which is apparent from the shape of the radial quark momentum distribution $|\mathbf{p}_b|\mathscr{G}(\mathbf{p}_b, -\mathbf{p}_b)$. In fact, the quark momentum distribution obtained in this model [69–71] is similar to the prediction of the QCD relativistic quark model analysis [72,73]. The rms value of the active quark momentum $\sqrt{\langle|\mathbf{p}_b^2|\rangle}$, where $\langle|\mathbf{p}_b^2|\rangle = \langle B_F(0)|\mathbf{p}_b^2|B_F(0)\rangle$, the expectation value of the binding energies of the active quark b, and spectator $\bar{q}$ and the sum of the binding energy of quark and antiquark pair $\langle E_b(\mathbf{p}_b^2)\rangle$, $\langle E_{\bar{q}}(|-\mathbf{p}_b^2|)\rangle$ and $\langle[E_b(\mathbf{p}_b^2) + E_{\bar{q}}(|-\mathbf{p}_b^2|)]\rangle$, respectively, calculated in the framework of RIQ model, are presented in Table 2.

Four important aspects of our present approach are noteworthy here. (1) The rms value of the quark momentum in the meson-bound state is much less than the corresponding upper bound $|\mathbf{p}_b|_{max}$, as expected. (2) The average energy of constituent quarks of the same flavor in different meson-bound states do not exactly match. This is because the kinematics and binding energy conditions for constituent quarks due to the color forces involved are different from one meson-bound state to another. The constituent quarks in the meson-bound state are considered to be free particles of definite momenta, each associated with its momentum probability amplitude derivable in this model via momentum space projection of the respective quark eigenmodes. On the other hand, the energies shown in Eqs. (27, 28), which are the energy eigenvalues of the corresponding bound quarks with no definite momenta of their own, are obtained from respective quark orbitals by solving the Dirac equation in this model. This makes a marginal difference between the energy eigenvalues (27, 28) and the average energy of constituent quarks shown in Table 2. (3) The expectation values of the sum of the energy of a constituent quark and antiquark in the meson-bound state are obtained in good agreement with the corresponding observed meson masses as shown in Table 2. These important aspects of our results lend credence to our energy conservation ansatz in an average sense through the effective momentum distribution function like $\mathscr{G}_{B_F}(\mathbf{p}_b, -\mathbf{p}_b)$ in the meson-bound state $|B_F(0)\rangle$. This ansatz along with three momentum conservation in the meson-bound state (A.1) ensures the required energy-momentum conservation in our description of several decay processes pointed out earlier. In the absence of any rigorous field theoretic description of the meson-bound states, invoking such an ansatz is no doubt a reasonable approach for a constituent-level description of hadronic phenomena. (4) Finally, in a self-consistent dynamical approach, we extract the form factors from the overlapping integrals of meson wave functions, where the q^2 dependence of the decay amplitude is automatically encoded. This is in contrast to some other model approaches cited in the literature where the form factors are determined only at one kinematic point, i.e., either at $q^2 \to 0$ or $q^2 \to q^2_{max}$, and then extrapolated to the entire kinematic range using some phenomenological ansatz (mainly dipole or Gaussian form).

The invariant form factors $g(q^2)$, $f(q^2)$ and $a_+(q^2)$, which represent the decay amplitudes, are found to have different dimensions. In order to study their q^2-dependence over the allowed kinematic range, they need to be treated on equal footing by casting them in the dimensionless form:

$$\begin{aligned} V(q^2) &= (M + m_{V_1})g(q^2), \\ A_1(q^2) &= (M + m_{V_1})^{-1} f(q^2), \\ A_2(q^2) &= -(M + m_{V_1})a_+(q^2). \end{aligned} \tag{31}$$

It is interesting to study the q^2-dependence of the dimensionless form factors in the present model in the allowed kinematic range. The q^2-dependence of the form factors into ground state mesons, (for example, $B \to D^*$ and

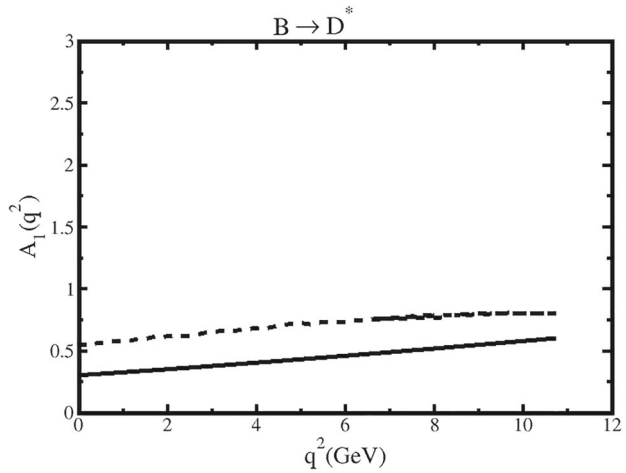

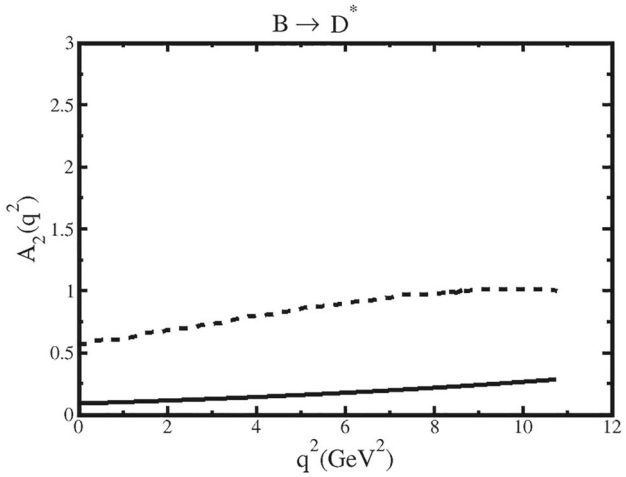

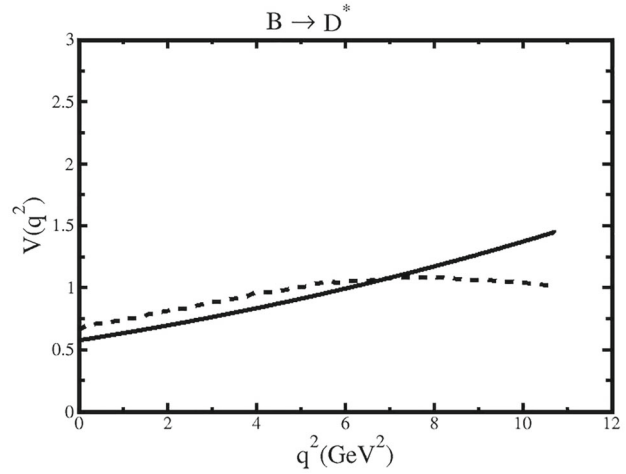

Fig. 2 Our predicted q^2-dependence of $B \to D^*$ form factors (solid curve) along with that of the pQCD + Lattice QCD approach (dotted curve)

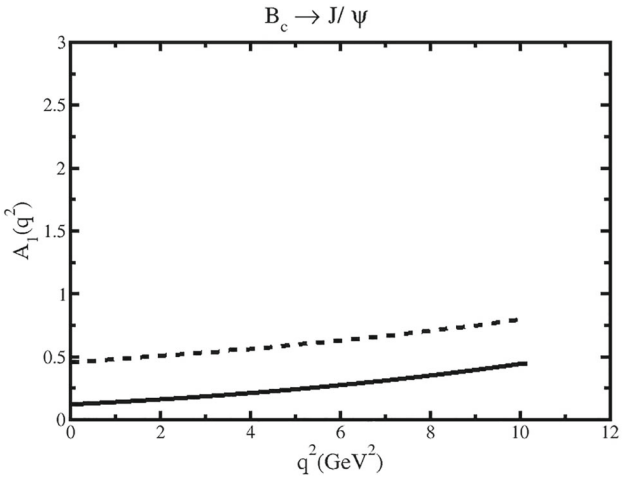

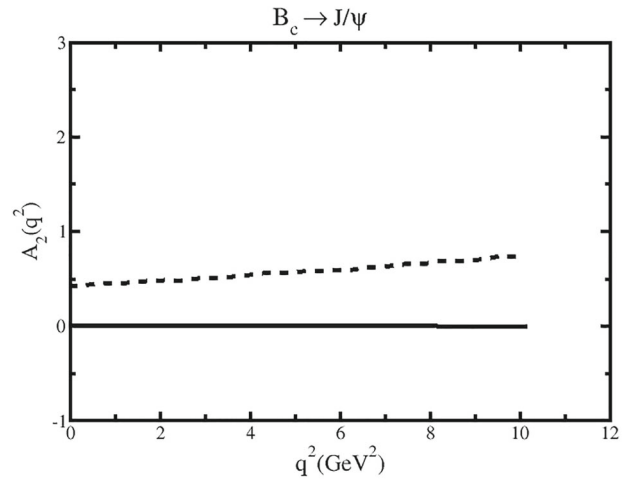

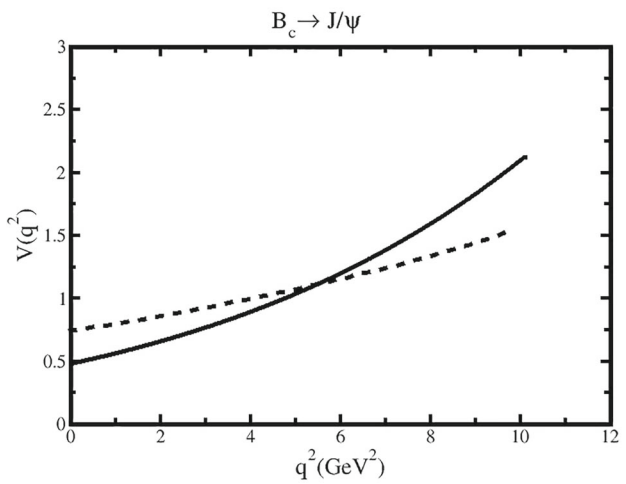

Fig. 3 Our predicted q^2-dependence of $B_c \to J/\psi$ form factors (solid curve) along with that of Lattice QCD approach (dotted curve)

$B_c \to J/\psi$) in the present model along with corresponding results obtained from pQCD + Lattice QCD [93] and Lattice QCD [94] approaches are shown in Figs. 2, 3. The nature and shape of our predicted q^2-dependence of form factors:

$A_1(q^2)$ and $A_2(q^2)$ are found similar but lying below the behavioural pattern obtained from results of Refs. [93,94] throughout the kinematic range. Our predicted $V(q^2)$ is, of course, found closer, but its behavioural pattern over

Table 3 Predicted form factors for decays to 1S state

Decay mode	Valued at	$V(q^2)$	$A_1(q^2)$	$A_2(q^2)$
$B_c^- \to J/\psi$	$q^2 = 0$	0.482	0.125	0.0095
	$q^2 = q^2_{max}$	2.121	0.452	0.0006
$B_c^- \to D_s^{*-}$	$q^2 = 0$	0.077	0.016	0.0192
	$q^2 = q^2_{max}$	4.584	0.466	0.8853
$B_c^- \to D^{*-}$	$q^2 = 0$	0.033	0.006	0.0105
	$q^2 = q^2_{max}$	6.527	0.403	1.5552
$B^- \to \rho^-$	$q^2 = 0$	0.073	0.056	0.0123
	$q^2 = q^2_{max}$	3.680	0.756	0.2041
$B^- \to K^{*-}$	$q^2 = 0$	0.155	0.123	0.0153
	$q^2 = q^2_{max}$	2.669	0.828	0.0191
$B^- \to D^{0*}$	$q^2 = 0$	0.578	0.307	0.0954
	$q^2 = q^2_{max}$	1.447	0.605	0.2885
$\bar{B^0} \to D^{*+}$	$q^2 = 0$	0.578	0.307	0.0953
	$q^2 = q^2_{max}$	1.448	0.604	0.2877
$\bar{B_s^0} \to D_s^{*+}$	$q^2 = 0$	0.523	0.254	0.0725
	$q^2 = q^2_{max}$	1.514	0.584	0.2674

the allowed kinematic range is obtained different from that of Refs. [93,94]. Starting with somewhat lesser value at $q^2 \to 0$, $V(q^2)$ in the present model increases with q^2 in the lower q^2-region till it equals with their results at $q^2 \simeq 7GeV^2$ for $B \to D^*$ [93] and at $q^2 \simeq 5.5GeV^2$ for $B_c \to J/\psi$ [94] form factor, respectively. Thereafter, our predicted $V(q^2)$ overshoots their results and increases faster in their respective higher q^2-region up to the point: $q^2 \to q^2_{max}$. Our predicted form factors, evaluated with fixed input parameters (27, 28) at kinematic points: maximum recoil point ($q^2 \to 0$) and minimum recoil point ($q^2 \to q^2_{max}$), are shown in Table 3. For comparison of our predictions with those of pQCD + Lattice QCD [93] and Lattice QCD [94], we also extract the uncertainties caused by the choice of the input parameters simultaneously within 10% of their central values and take the largest variation as the uncertainty [95]. One can see that our predicted $V(q^2)$ and $A_1(q^2)$ at $q^2 \to 0$ and $q^2 \to q^2_{max}$ are comparable to those of Ref. [93,94] shown in Table 4. However, $A_2(q^2)$ at two extreme kinematic points are found underestimated compared to their results. Our predictions of $B \to D^*$ form factors with uncertainties are: $V(q^2 \to 0) = 0.578 \pm 0.05$, $A_1(q^2 \to 0) = 0.307 \pm 0.048$, $A_2(q^2 \to 0) = 0.095 \pm 0.038$, $V(q^2 \to q^2_{max}) = 1.447 \pm 0.009$, $A_1(q^2 \to q^2_{max}) = 0.605 \pm 0.055$, $A_2(q^2 \to q^2_{max}) = 0.288 \pm 0.079$ and those of $B_c \to J/\psi$ form factors are: $V(q^2 \to 0) = 0.482 \pm 0.072$, $A_1(q^2 \to 0) = 0.125 \pm 0.029$, $A_2(q^2 \to 0) = 0.009 \pm 0.002$, $V(q^2 \to q^2_{max}) = 2.121 \pm 0.002$, $A_1(q^2 \to q^2_{max}) = 0.452 \pm 0.044$, $A_2(q^2 \to q^2_{max}) = 0.0006 \pm 0.0001$. This indicates that our predictions on $B \to D^*$ and $B_c \to J/\psi$ form factors are reasonable in comparison with the pQCD + Lattice QCD and Lattice QCD results. Our predicted form factors at $q^2 \to 0$ and $q^2 \to q^2_{max}$ for transition of $\bar{B}^0$, $\bar{B}^0_s$, B^- and B_c^--mesons to radially excited ($2S$ and $3S$) states are shown in Tables 5, and 6.

One may naively expect the form factor in the dimensionless form to satisfy the heavy quark-symmetry (HQS) relation:

$$V(q^2) \simeq A_2(q^2) \simeq \tilde{A}_1(q^2), \tag{32}$$

as an outcome of the heavy quark effective theory (HQET), where

$$\tilde{A}_1(q^2) = \left[1 - \frac{q^2}{(M + m_{V_1})^2}\right]^{-1} A_1(q^2). \tag{33}$$

With the input parameters (27, 28), we first study the q^2-dependence of the dimensionless form factors in their allowed kinematic ranges. Our predictions do not entirely agree with HQS relation. This is due to the well-known fact that the heavy flavor symmetry is not strictly applicable in the heavy meson sector, particularly when two heavy constituent quarks are involved. The q^2-dependence of form factors for B_c^-, B^-, $\bar{B}^0$, $\bar{B}^0_s$-decays to S-wave charmonium, charm, strange and non-strange light meson states in the present model is shown in the Figs. 4, 5, 6, 7, 8, 9, and 10. We find that the departure from HQS relation is more pronounced in the decays to higher and higher excited states. This is due to different kinematics and four-momentum transfer involved in different decay modes.

Before predicting the physical quantities of interest: decay width and branching fraction etc., it is interesting to go for a qualitative assessment of transition probabilities for transition to different S-wave states. For this, we study the radial quark momentum distribution amplitude $|\mathbf{p}_q|\mathcal{G}_{B_F}(\mathbf{p}_q, -\mathbf{p}_q)$

Table 4 $B \to D^*$ and $B_c \to J/\psi$ form factors from pQCD + Lattice QCD and Lattice QCD results

Decay mode	Valued at	$V(q^2)$	$A_1(q^2)$	$A_2(q^2)$	Reference
$B \to D^*$	$q^2 \to 0$	0.671	0.556	0.584	[93]
	$q^2 \to q^2_{max}$	1.01 ± 0.02	0.81 ± 0.02	1.01 ± 0.02	[93]
$B_c \to J/\psi$	$q^2 \to 0$	$0.742^{+0.052}_{-0.064}$	$0.461^{+0.027}_{-0.026}$	$0.433^{+0.095}_{-0.10}$	[94]
	$q^2 \to q^2_{max}$	$1.536^{+0.105}_{-0.058}$	$0.792^{+0.032}_{-0.023}$	$0.737^{+0.124}_{-0.071}$	[94]

Table 5 Predicted form factors for decays to 2S state

Decay mode	Valued at	$V(q^2)$	$A_1(q^2)$	$A_2(q^2)$
$B_c^- \to \psi(2S)$	$q^2 = 0$	0.245	0.048	0.022
	$q^2 = q^2_{max}$	1.829	0.314	0.155
$B_c^- \to D_s^{*-}(2S)$	$q^2 = 0$	0.066	0.010	0.019
	$q^2 = q^2_{max}$	3.961	0.325	1.087
$B_c^- \to D^{*-}(2S)$	$q^2 = 0$	0.046	0.006	0.015
	$q^2 = q^2_{max}$	5.789	0.300	1.869
$B^- \to D^{0*}(2S)$	$q^2 = 0$	0.273	0.094	0.019
	$q^2 = q^2_{max}$	1.231	0.357	0.097
$\bar{B^0} \to D^{*+}(2S)$	$q^2 = 0$	0.265	0.094	0.020
	$q^2 = q^2_{max}$	1.224	0.363	0.106
$\bar{B_s^0} \to D_s^{*+}(2S)$	$q^2 = 0$	0.252	0.084	0.014
	$q^2 = q^2_{max}$	1.287	0.360	0.090

Table 6 Predicted form factors for decays to 3S state

Decay mode	Valued at	$V(q^2)$	$A_1(q^2)$	$A_2(q^2)$
$B_c^- \to \psi(3S)$	$q^2 = 0$	0.1121	0.0198	0.0015
	$q^2 = q^2_{max}$	1.5727	0.2383	0.0015
$B_c^- \to D_s^{*-}(3S)$	$q^2 = 0$	0.0286	0.0036	0.0014
	$q^2 = q^2_{max}$	3.6723	0.2490	0.0014
$B_c^- \to D^{*-}(3S)$	$q^2 = 0$	0.0213	0.0022	0.0014
	$q^2 = q^2_{max}$	5.3214	0.2283	0.0014
$B^- \to D^{0*}(3S)$	$q^2 = 0$	0.1177	0.0337	0.0034
	$q^2 = q^2_{max}$	1.1429	0.2742	0.0020
$\bar{B^0} \to D^{*+}(3S)$	$q^2 = 0$	0.1203	0.0339	0.0029
	$q^2 = q^2_{max}$	1.1469	0.2716	0.0044
$\bar{B_s^0} \to D_s^{*+}(3S)$	$q^2 = 0$	0.1143	0.0307	0.0009
	$q^2 = q^2_{max}$	1.1360	0.2569	0.0176

of the parent and daughter mesons over the physical range of respective quark momentum $\mathbf{p}_q$, for each such decay mode. From the plot shown in Figs. 11, 12, the overlap region between the momentum distribution profile of the parent and daughter meson in the transition to the $1S$ state is found to be maximum and it decreases for transitions to higher excited $2S$ and $3S$ states. Since the invariant form factors are evaluated from overlapping integrals of participating meson wave functions, it is expected that the contribution of the form factors to decay width/ branching fractions should be in decreasing order of magnitude, going from decays to $1S$ state to higher excited ($2S$ and $3S$) states.

We calculate the decay width from the expression (26) via (14) and (9, 10). Our predicted decay widths $\Gamma(B_F \to V_1(nS)V_2)$ for general values of QCD coefficients (a_1, a_2) of the operator product expansion are listed in Table 7 to facilitate a comparison with other dynamical model predictions. The branching fractions (BFs) for B_c^-, $\bar{B_s^0}$, B^-, $\bar{B^0}$-decays to $1S$, $2S$ and $3S$ charmonium, charm, strange and non-strange meson states, are predicted in reasonable agreement with available experimental data [87] and other model predictions, as shown in Tables 8, 9, 10, respectively.
Our results for BFs of decays to $1S$, $2S$ and $3S$ states corresponding to 3 sets of QCD parameters are listed in the second column of each table. As expected, our predicted branching fractions are obtained in the hierarchy:

$$\mathscr{B}(B_F \to V_1(3S)V_2) < \mathscr{B}(B_F \to V_1(2S)V_2) < \mathscr{B}(B_F \to V_1(1S)V_2).$$

Our results for transitions to $2S$ and $3S$ states are found two and three orders of magnitude down compared to those obtained for transition to $1S$ state. The node structure of the $2S$ wave function is responsible for small BFs. Since there is no node for the initial wave function, the contribution from the positive and negative parts of the final wave function cancel each other out yielding small BFs. In case of transition to $3S$ states, there are even more serious cancellations; leading to still smaller BFs. As expected, the tighter phase space and the q^2-dependence of the form factors typical to the decay mode lead to smaller BFs for transitions to higher excited $2S$ and still smaller for the transition of $3S$ states.

The BFs of the decay modes, considered in the present study, are obtained in a wide range of $\sim 10^{-2}$ to 10^{-6}. For nonleptonic B_F-meson decays to 1S, 2S, and 3S final meson states, BFs range from $\sim 10^{-2}$ to 10^{-3}, $\sim 10^{-4}$ to 10^{-5} and $\sim 10^{-5}$ to 10^{-6}, respectively. The dominant decay modes: $B_c^- \to J/\psi D_s^{*-}$, $\bar{B_s^0} \to D_s^{*+}\rho^-$, $\bar{B^0} \to D^{*+}\rho^-$, $B^- \to D^{*0}\rho^-$ and $B^- \to K^{*-}J/\psi$ are found to have BFs of 0.27, 1.16, 1.40, 1.52 and 0.46, respectively in $\mathscr{O}(\sim 10^{-2})$ which should be experimentally accessible. For such decays to corresponding $2S$ modes, the predicted BFs, of 0.44, 11.16,

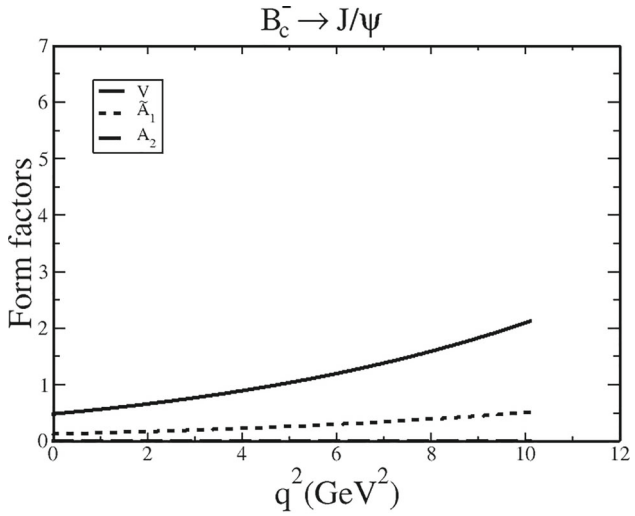

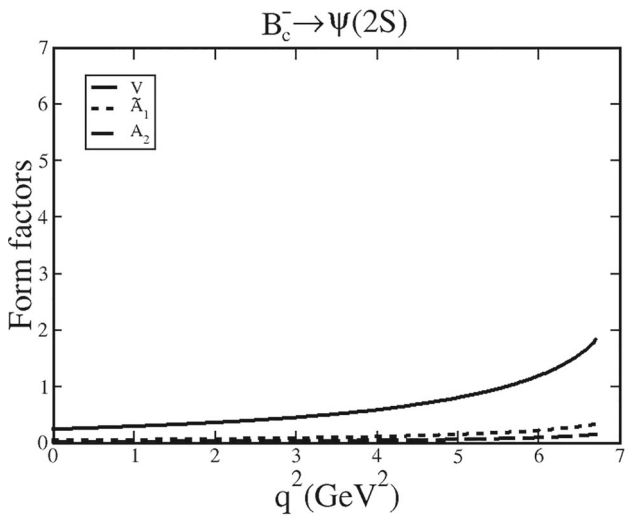

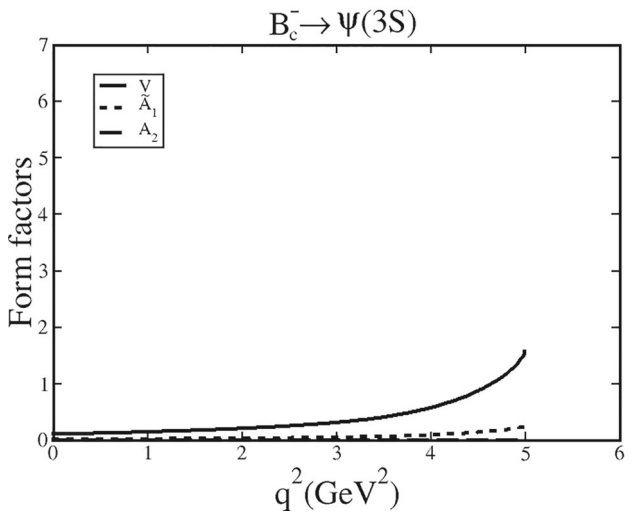

Fig. 4 q^2-dependence of $B_c^- \to \psi(nS)$ transition form factors

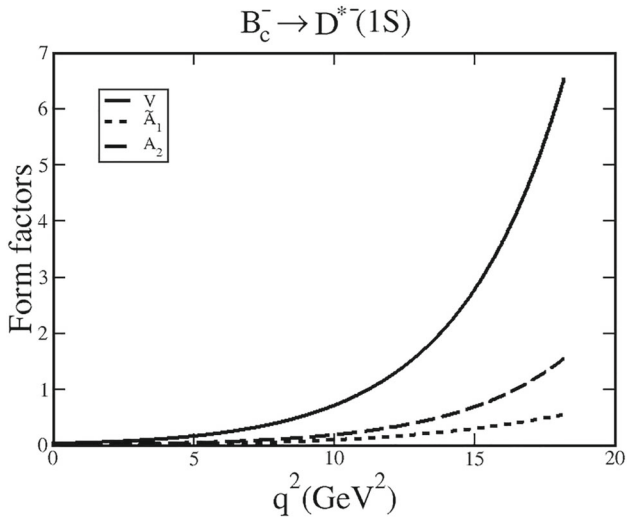

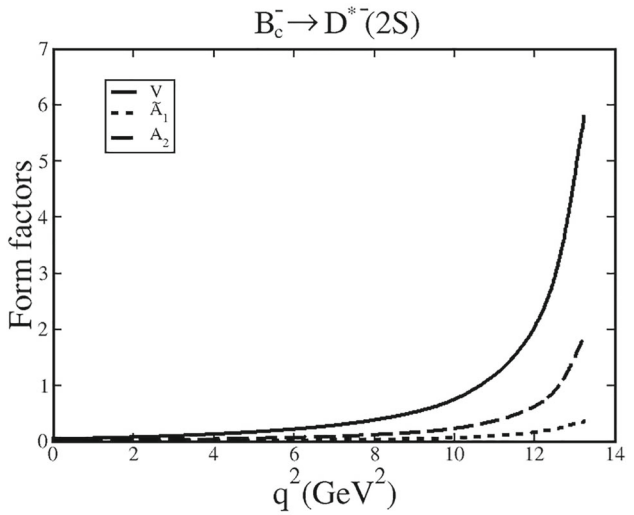

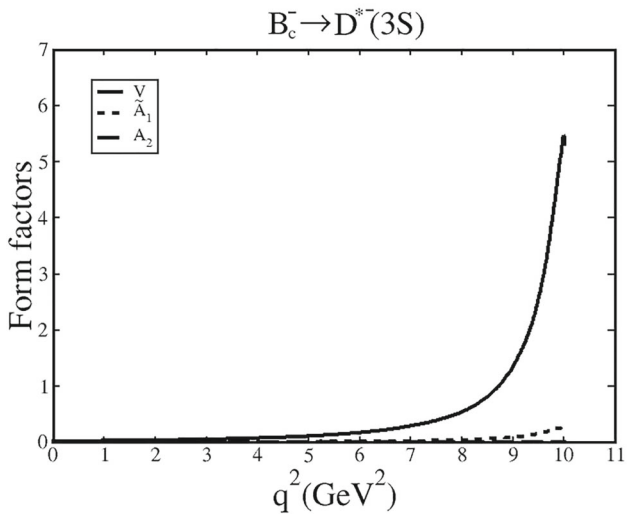

Fig. 5 q^2-dependence of $B_c^- \to D^{*-}(nS)$ transition form factors

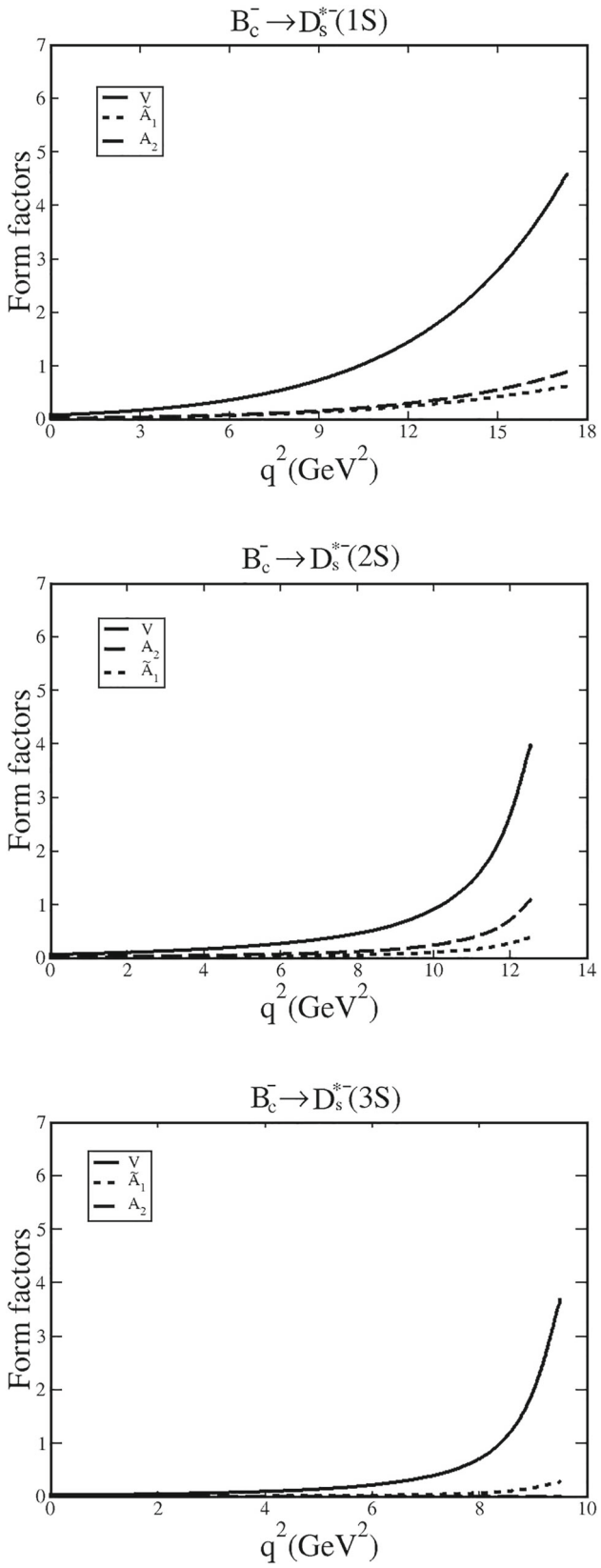

Fig. 6 q^2-dependence of $B_c^- \to D_s^{*-}(nS)$ transition form factors

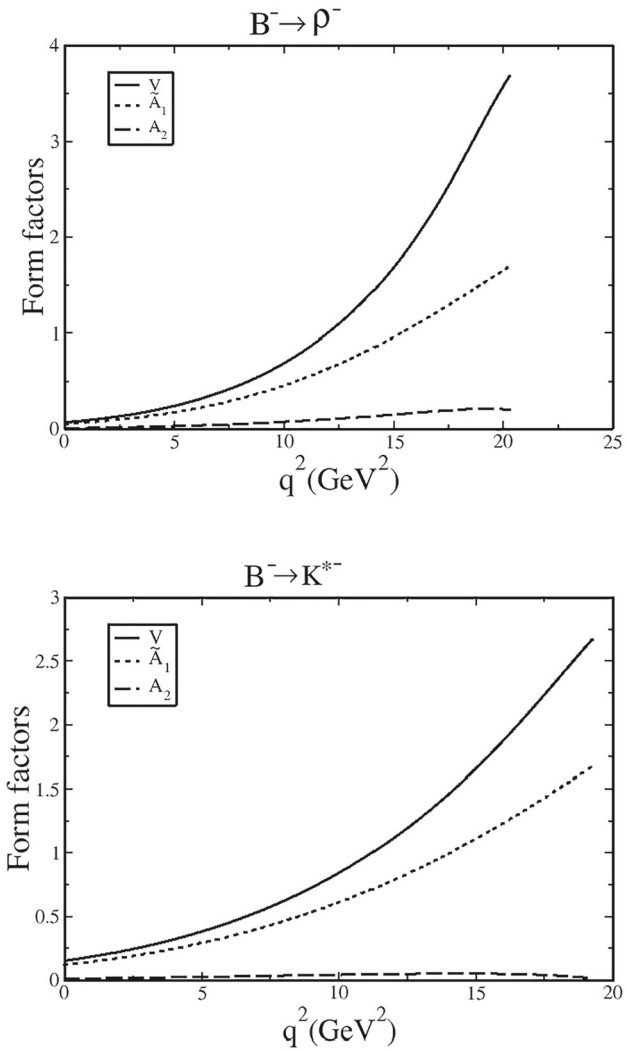

Fig. 7 q^2-dependence of $B^- \to \rho^-$ and $B^- \to K^{*-}$ transition form factors

11.01, 11.65 and 24.50 in $\mathcal{O}(\sim 10^{-4})$, lie within the detection accuracy of current experiments. The neutral B-meson decay in the present study is found to have smaller BFs than those of charged B-meson decays, as expected. This may be due to the spectator interaction effects of d and u quarks.

Our predicted BFs for general values of QCD parameters (a_1, a_2) in B^-, $\bar{B}^0$ and $\bar{B}_s^0$ decays to two charmful $(1S, 2S, 3S)$ states, obtained in $\mathcal{O}(10^{-2}-10^{-4})$, are shown in Table 11 and those for $B_c^- \to D_{(s)}^{*-} D^{*0}$, $\bar{D}^{*0} D_{(s)}^{*-}$, obtained in $\mathcal{O}(10^{-6})$ are, shown in Tables 12, 13. Our predictions in this sector are, of course, found somewhat underestimated compared to those of Ref. [24] and available experimental data [87].

The relative size of BFs for nonleptonic decays is broadly estimated from a power counting of QCD factors: (a_1, a_2) in the Wolfenstein parameterization [96]. Accordingly, class I decays determined by a_1 are found to have comparatively

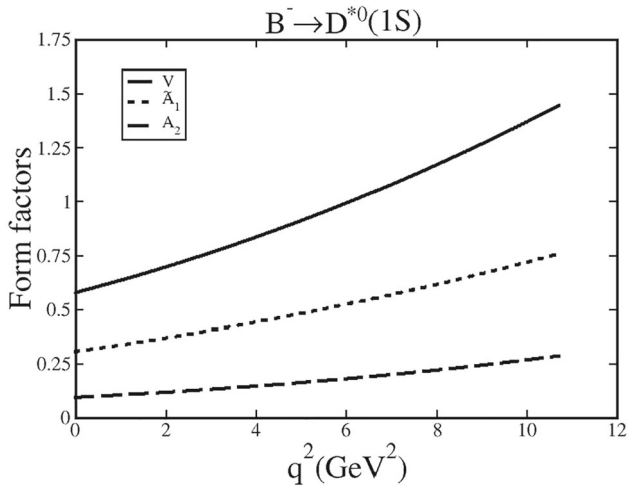

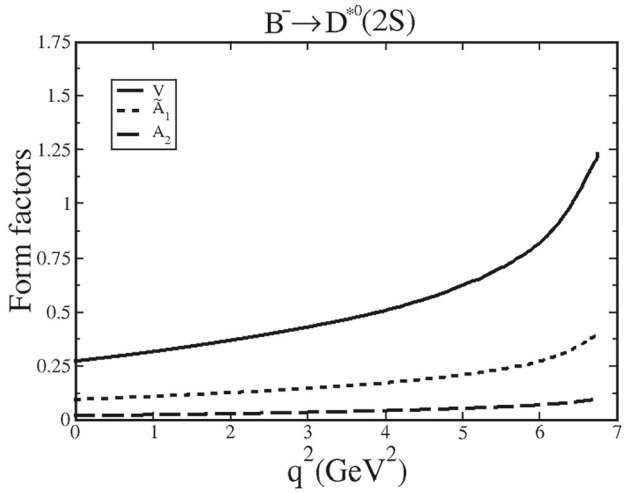

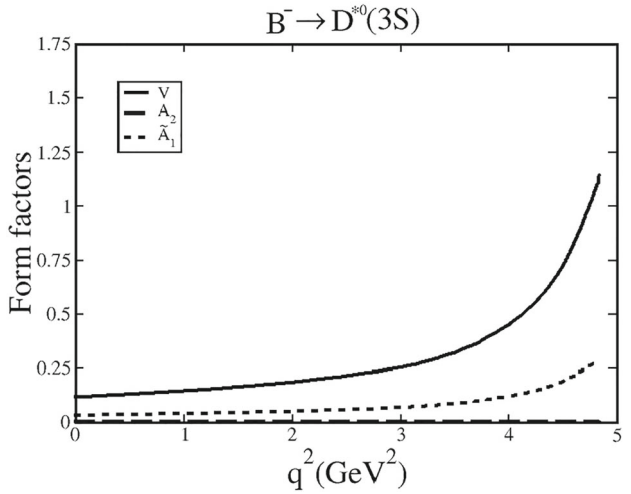

Fig. 8 q^2-dependence of $B^- \to D^{*0}(nS)$ transition form factors

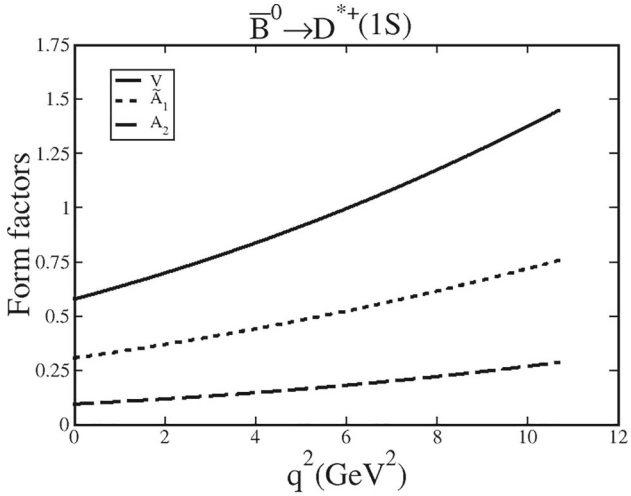

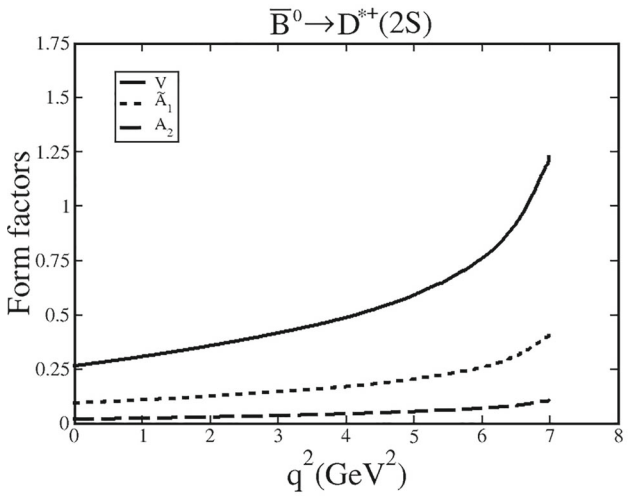

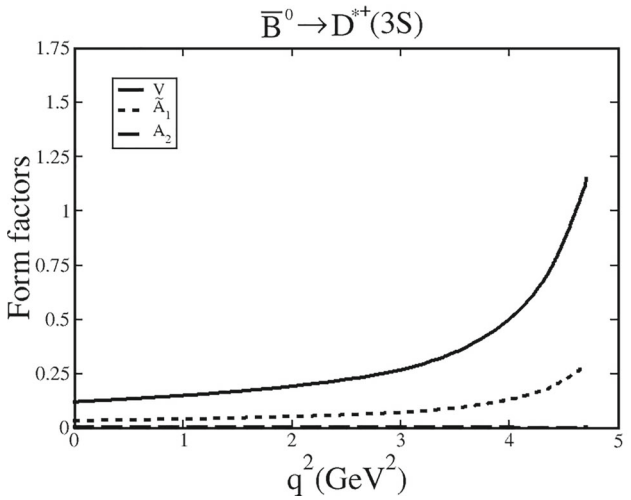

Fig. 9 q^2-dependence of $\bar{B^0} \to D^{*+}(nS)$ transition form factors

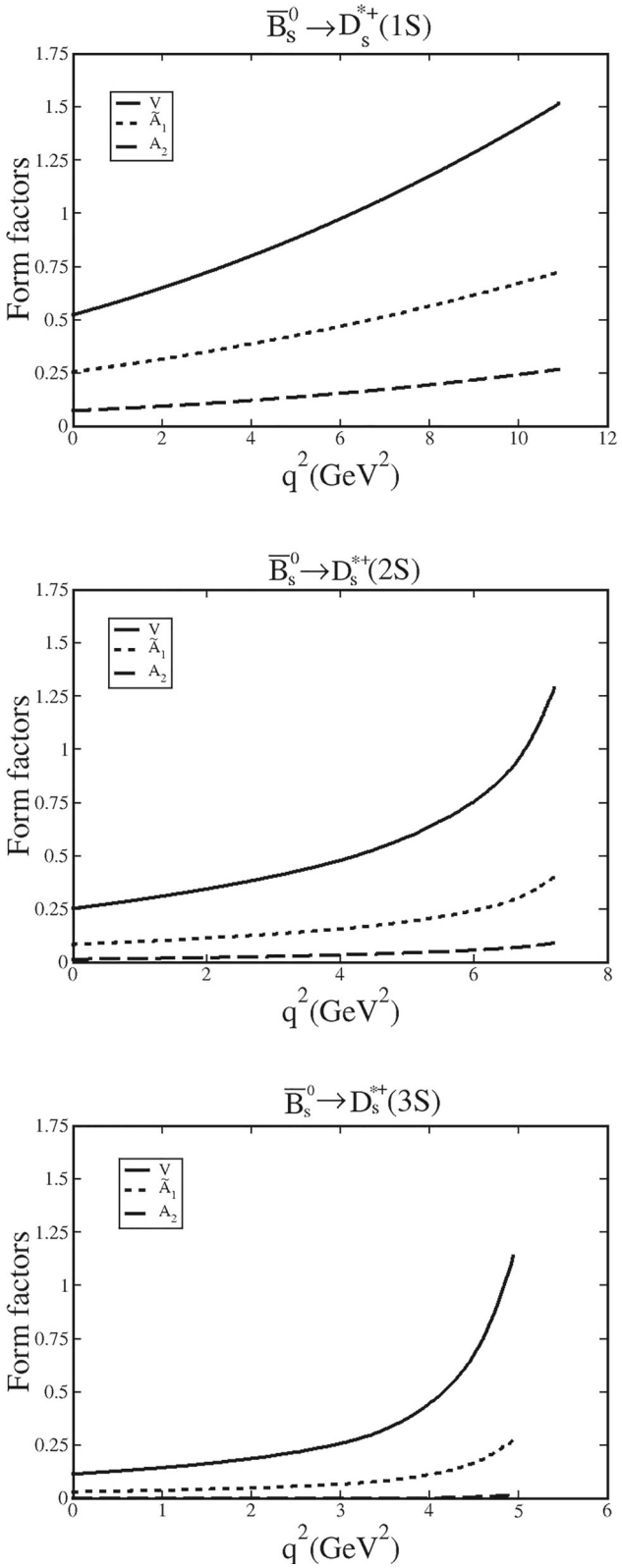

Fig. 10 q^2-dependence of $\bar{B}_s^0 \to D_s^{*+}(nS)$ transition form factors

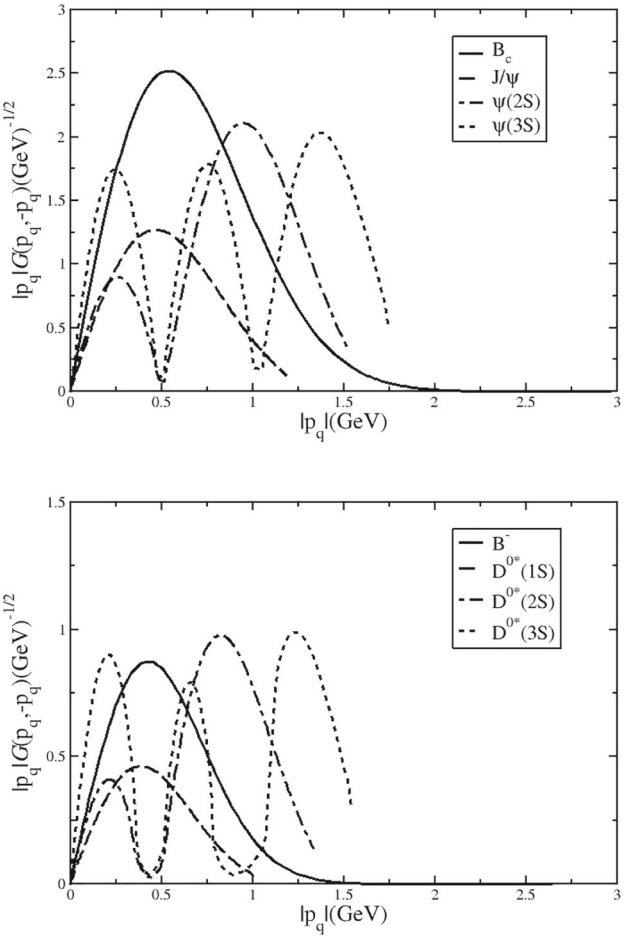

Fig. 11 Overlap of momentum distribution amplitudes of the initial and final meson states

large BFs as shown in Tables 8, 9, 10. On the other hand, class II decay modes, determined by a_2, are found to have relatively small BFs, as expected, except for decay modes: $B^- \to K^{*-}J/\psi$ and $B^- \to K^{*-}\psi(2S)$, characterized by a product of CKM factors: $V_{bc}V_{cs}$, with predicted BFs $\sim 0.27\%$ and 0.14%, respectively. These modes should be measured at high luminosity hadron colliders. In class III decay modes that are characterized by Pauli interference, the BFs are determined by the relative value of a_1 with respect to a_2. Considering positive values of $a_1 = 1.12$ and negative value of $a_2 = -0.26$ in Set 1, for example, which leads to destructive interference, the decay modes are suppressed compared to the case where interference is switched off. However, at a qualitative level, where the ratio $\frac{a_2}{a_1}$, a function of running coupling constant α_S evaluated at the factorization scale, is shown to be positive in the case of b-flavored meson decays corresponding to small coupling [33]. The experimental data also favor constructive interference of the color-favored and color-suppressed b-flavored meson decay modes. Considering positive value of $a_2^b = 0.26$, our predicted BFs of class III decay modes: $B_c^- \to J/\psi D_s^{*-}$

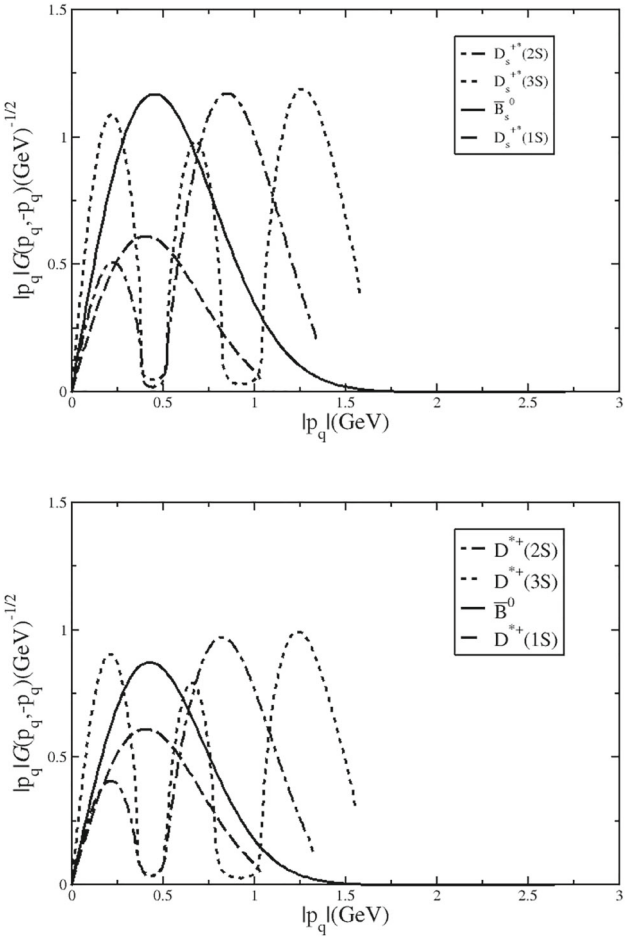

Fig. 12 Overlap of momentum distribution amplitudes of the initial and final meson states

and $B_c^- \to \psi(2S)D_s^{*-}$ for example, find enhancement by a factor of ~ 2 and ~ 77, respectively, over that obtained with $a_2 = -0.26$. For decay modes to $3S$ states, the enhancement is still more significant.

In the spirit of the experimental data favoring a constructive interference of the color-favored and color-suppressed b-flavored meson decays, the effect of Pauli interference inducing enhancement of BFs can be further probed by casting the decay width (Γ) in the form: $\Gamma = \Gamma_0 + \Delta\Gamma$, where $\Gamma_0 = x_1^2 a_1^2 + x_2^2 a_2^2$, $\Delta\Gamma = 2x_1 x_2 a_1 a_2$ and then evaluating $\frac{\Delta\Gamma}{\Gamma_0}$ in each case as done in [34–41,56]. We find that the absolute values of $\frac{\Delta\Gamma}{\Gamma_0}$ for $B_c^- \to J/\psi D_s^{*-}$, $B_c^- \to \psi(2S)D_s^{*-}$, $B_c^- \to J/\psi D^{*-}$ and $B_c^- \to \psi(2S)D^{*-}$ (in %) are ~ 56, ~ 97, ~ 33, and ~ 99, respectively. For B_c-decays to two charmful states: $B_c^- \to \bar{D}^{*0}D_s^{*-}$ and $B_c^- \to \bar{D}^{*0}D^{*-}$, the enhancement in % is found to be ~ 4 and ~ 3, respectively. This indicates that interference is less significant in $B_c^- \to \bar{D}^{*0}D_{(s)}^{*-}$ compared to that obtained for B_c-decays to charmonium and charm meson final states. However, the B_c-meson decays to two charmful vector meson ($\bar{D}^{*0}D_{(s)}^{*-}$) states are particularly important as these decay modes are proposed for extraction of the CKM angle γ through amplitude relation [97–100].

The nonleptonic decays of b-flavored mesons to two charmful vector meson states, characterized by charge conjugation symmetry of the final states, are of special interest. It is important to predict the observables: CP-odd fraction ($R_\perp$) and longitudinal polarization fraction (R_L), which are expressed in terms of helicity amplitudes (10) in the form:

$$R_\perp = \frac{|\mathscr{A}_\pm - \mathscr{A}_\mp|^2}{2[|\mathscr{A}_\pm|^2 + |\mathscr{A}_\mp|^2 + |\mathscr{A}_{ll}|^2]},$$
$$R_L = \frac{|\mathscr{A}_{ll}|^2}{[|\mathscr{A}_\pm|^2 + |\mathscr{A}_\mp|^2 + |\mathscr{A}_{ll}|^2]}. \quad (34)$$

The predicted $R_\perp$ in B_c-decays to two charmful states in the present model are obtained one order of magnitude higher than those in other b-flavored meson decays as shown in Table 14. For color-favored $B_c^- \to D^* D_{(s)}^{*-}$ decays, the effect arising due to the short-distance non-spectator contribution is shown to be marginal [101]. However, the long-distance (LD) nonfactorizable contributions from rescattering effects, final-state interactions, etc., may not be negligible. If a significant LD effect exists, one expects large CP-odd fractions in these decays. Our predicted $R_\perp$ for $B \to D^* D_{(s)}^*$ decay modes, in particular, are of course found slightly smaller than other model predictions [102,103]. This is due to large helicity amplitude $\mathscr{A}_{ll}$ and small value of the form factor $g(q^2)$ obtained in the present model. Our predictions for $R_\perp$ in other b-flavored (B_c, B^-, $\bar{B}^0$, $\bar{B}_{(s)}^0$) meson decays to final vector meson states involving any two in the charmonium, charm and light vector meson sector are listed in Table 15. Among all such decay modes, $B_c^- \to \psi(nS)D_{(s)}^{*-}$ and $B^- \to \rho^-(K^{*-})\psi(nS)$ are found to have significant CP-odd fractions. In all decay modes considered in the present analysis, the predicted longitudinal polarization fractions shown in Tables 14, 15 dominate over corresponding CP-odd fractions as expected from the naive counting rules.

5 Summary and conclusion

In this work, we study the exclusive two-body nonleptonic decays of b-flavored ($\bar{B}^0$, $\bar{B}_s^0$, B^- and B_c^-) mesons to S-wave charmonium and charm meson 1^- states, in the framework of relativistic independent quark (RIQ) model. The weak decay form factors representing decay amplitude and their q^2-dependence are extracted from the overlapping integrals of the meson wave functions obtainable in the RIQ model. The predicted branching fractions for different decay modes are obtained in a wide range, from $\mathscr{O}(10^{-6})$ for B_c^- decays to two charmful states to as high as $\sim 1.52\%$, $\sim 1.40\%$ and $\sim 1.16\%$ for $B^- \to D^{*0}\rho^-$, $\bar{B}^0 \to D^{*+}\rho^-$ and

Table 7 Decay widths in units of 10^{-15} GeV in terms of Wilson coefficients a_1 and a_2

$B_c^- \to J/\psi X^-$	Width	$B_c^- \to \psi(2S)X^-$	Width	$B_c^- \to \psi(3S)X^-$	Width
ρ^-	$1.8299a_1^2$	ρ^-	$0.2046a_1^2$	ρ^-	$0.0262a_1^2$
K^{*-}	$0.0978a_1^2$	K^{*-}	$0.0111a_1^2$	K^{*-}	$0.0014a_1^2$
D_s^{*-}	$(2.413a_1 + 3.199a_2)^2$	D_s^{*-}	$(1.0389a_1 + 3.557a_2)^2$	D_s^{*-}	$(0.675a_1 + 1.910a_2)^2$
D^{*-}	$(0.438a_1 + 0.320a_2)^2$	D^{*-}	$(0.179a_1 + 0.703a_2)^2$	D^{*-}	$(0.110a_1 + 0.462a_2)^2$
$\bar{B}_s^0 \to D_s^{*+}(1S)X^-$	Width	$\bar{B}_s^0 \to D_s^{*+}(2S)X^-$	Width	$\bar{B}_s^0 \to D_s^{*+}(3S)X^-$	Width
ρ^-	$3.886a_1^2$	ρ^-	$0.3482a_1^2$	ρ^-	$0.0353a_1^2$
K^{*-}	$0.203a_1^2$	K^{*-}	$0.0186a_1^2$	K^{*-}	$0.0019a_1^2$
$\bar{B}^0 \to D^{*+}(1S)X^-$	Width	$\bar{B}^0 \to D^{*+}(2S)X^-$	Width	$\bar{B}^0 \to D^{*+}(3S)X^-$	Width
ρ^-	$4.8481a_1^2$	ρ^-	$0.3805a_1^2$	ρ^-	$0.0362a_1^2$
K^{*-}	$0.2512a_1^2$	K^{*-}	$0.0202a_1^2$	K^{*-}	$0.0019a_1^2$
$B^- \to D^{*0}(1S)X^-$	Width	$B^- \to D^{*0}(2S)X^-$	Width	$B^- \to D^{*0}(3S)X^-$	Width
ρ^-	$4.860a_1^2$	ρ^-	$0.3733a_1^2$	ρ^-	$0.0365a_1^2$
K^{*-}	$0.2511a_1^2$	K^{*-}	$0.0199a_1^2$	K^{*-}	$0.0020a_1^2$
$B^- \to X^- J/\psi$	Width	$B^- \to X^-\psi(2S)$	Width	$B^- \to X^-\psi(3S)$	Width
ρ^-	$0.913a_2^2$	ρ^-	$0.571a_2^2$	ρ^-	$0.187a_2^2$
K^{*-}	$27.31a_2^2$	K^{*-}	$14.58a_2^2$	K^{*-}	$4.778a_2^2$

Table 8 Branching fractions in % for three sets of values of Wilson coefficients a_1 and a_2

$B_c^- \to J/\psi X^-$	Branching fraction $a_1 = 1.12$ $a_2 = -0.26$	$a_1 = 1.14$ $a_2 = -0.20$	$a_1 = 0.93$ $a_2 = -0.27$		[21]	[24]	[26]	[50]	[92]	
ρ^-	0.1778	0.1842	0.1226		0.16	0.49	–	0.40	–	
K^{*-}	0.0095	0.0098	0.0065		0.01	0.028	0.0109 ± 0.0033	0.022	–	
D_s^{*-}	0.2712	0.345	0.147			0.97	0.412 ± 0.123	0.67	0.78	
D^{*-}	0.0128	0.0146	0.0079			0.045	0.0182 ± 0.0055	0.028	0.031	
$\bar{B}_s^0 \to D_s^{*+}(1S)X^-$		Branching fraction		[19]						Experiment [87]
ρ^-	1.1606	1.2025	0.8002	$0.726^{+0.076}_{-0.071}$						0.96 ± 0.21
K^{*-}	0.0605	0.0627	0.0418	$0.0688^{+0.0067}_{-0.0064}$						
$\bar{B}^0 \to D^{*+}(1S)X^-$		Branching fraction		[19]						Experiment [87]
ρ^-	1.4034	1.4539	0.9676	$0.873^{+0.078}_{-0.073}$						0.68 ± 0.09
K^{*-}	0.0727	0.0753	0.0501	$0.0758^{+0.0064}_{-0.0059}$						0.033 ± 0.006
$B^- \to D^{*0}(1S)X^-$		Branching fraction		[19]						Experiment [87]
ρ^-	1.5171	1.5718	1.0460	$0.873^{+0.079}_{-0.073}$						0.98 ± 0.17
K^{*-}	0.0786	0.0814	0.0542	$0.0846^{+0.0070}_{-0.0064}$						0.081 ± 0.014
$B^- \to X^- J/\psi$		Branching fraction								Experiment [87]
ρ^-	0.015	0.009	0.0165							0.0041 ± 0.0005
K^{*-}	0.459	0.271	0.4914							0.143 ± 0.008

$\bar{B}_s^0 \to D_s^{*+}\rho^-$, respectively. Our results are in general agreement with the available experimental data and other SM predictions. The decay modes with predicted branching fractions in $\mathcal{O}(10^{-2})$, which include the B_c-meson decays to $1S$ charmonium and charm meson states as well as $\bar{B}^0$, B^- decays to two charmful mesons in their ground state, should be experimentally accessible. The decay modes to $2S$ and $3S$ charmonium states such as $B_c^- \to \psi(2S)\rho^-, \psi(2S)D_s^{*-}$, $\bar{B}_s^0 \to D_s^{*+}(2S)\rho^-$, $\bar{B}^0 \to D^{*+}(2S)\rho^-$, $B^- \to D^{*0}(2S)\rho^-$, $B^- \to K^{*-}\psi(2S)$, $B^- \to \rho^-\psi(2S)$ and $\bar{B}_s^0 \to D_s^{*+}(3S)\rho^-$, $\bar{B}^0 \to D^{*+}(3S)\rho^-$, $B^- \to D^{*0}(3S)\rho^-$, $B^- \to K^{*-}\psi(3S)$, $B^- \to \rho^-\psi(3S)$ with predicted branching fractions upto $\sim 10^{-4}$ may be accessible at high luminosity hadron colliders. Other decay modes and especially

Table 9 Branching fractions in 10^{-4} for three sets of values of Wilson coefficients a_1 and a_2

$B_c^- \to \psi(2S)X^-$	Branching fraction			[16]	[19]	[21]	[26]
	$a_1 = 1.12$ $a_2 = -0.26$	a_1=1.14 $a_2 = -0.20$	$a_1 = 0.93$ $a_2 = -0.27$				
ρ^-	1.98	2.06	1.37	5.69	$4.04^{+0.21}_{-0.17}$	1.8	
K^{*-}	0.108	0.112	0.074	0.304	$0.2822^{+0.0156}_{-0.0126}$	1.0	0.439 ± 0.071
D_s^{*-}	0.440	1.732	0.0024				8.85 ± 2.54
D^{*-}	0.0026	0.032	0.0039				0.432 ± 0.117
$\bar{B_s^0} \to D_s^{*+}(2S)X^-$		Branching fraction			[19]		[27]
ρ^-	11.16	11.56	7.69		$0.475^{+0.164}_{-0.121}$		22
K^{*-}	0.56	0.58	0.38		$0.0332^{+0.0122}_{-0.0090}$		1.2
$\bar{B^0} \to D^{*+}(2S)X^-$		Branching fraction			[19]		
ρ^-	11.01	11.41	7.59		$0.267^{+0.081}_{-0.061}$		
K^{*-}	0.58	0.61	0.40		$0.0162^{+0.0050}_{-0.0038}$		
$B^- \to D^{*0}(2S)X^-$		Branching fraction			[19]		
ρ^-	11.65	12.07	8.03		$0.287^{+0.088}_{-0.066}$		
K^{*-}	0.62	0.64	0.43		$0.0173^{+0.0054}_{-0.0041}$		
$B^- \to X^-\psi(2S)$		Branching fraction					Experiment [87]
ρ^-	0.96	0.56	1.03				
K^{*-}	24.50	14.50	26.46				6.7 ± 1.4

Table 10 Branching fractions in 10^{-5} for three sets of values of Wilson coefficients a_1 and a_2

$B_c^- \to \psi(3S)X^-$	Branching fraction			[19]
	$a_1 = 1.12$ $a_2 = -0.26$	$a_1 = 1.14$ $a_2 = -0.20$	$a_1 = 0.93$ $a_2 = -0.27$	
ρ^-	2.5	2.6	1.7	$3.35^{+0.78}_{-0.68}$
K^{*-}	0.14	0.15	0.09	$0.229^{+0.055}_{-0.045}$
D_s^{*-}	5.21	11.87	0.97	
D^{*-}	0.007	0.008	0.007	
$\bar{B_s^0} \to D_s^{*+}(3S)X^-$		Branching fraction		[19]
ρ^-	10.56	10.94	7.28	$3.55^{+0.88}_{-0.69}$
K^{*-}	0.580	0.601	0.40	$0.251^{+0.061}_{-0.048}$
$\bar{B^0} \to D^{*+}(3S)X^-$		Branching fraction		[19]
ρ^-	10.49	10.87	7.23	$1.03^{+0.44}_{-1.04}$
K^{*-}	0.576	0.597	0.39	$0.0709^{+0.0310}_{-0.0719}$
$B^- \to D^{*0}(3S)X^-$		Branching fraction		[19]
ρ^-	11.42	11.83	7.87	$1.11^{+0.50}_{-1.12}$
K^{*-}	0.63	0.65	0.43	$0.0753^{+0.0347}_{-0.0766}$
$B^- \to X^-\psi(3S)$		Branching fraction		
ρ^-	3.13	1.86	3.39	
K^{*-}	80.3	47.5	86.67	

B_c-decay to two charmful states with predicted branching factions in $\mathcal{O}(10^{-6} - 10^{-9})$ can not reach the detection ability of the current experiments. As expected, our predicted branching fractions are obtained in the hierarchy:

$$\mathscr{B}(B_F \to V_1(3S)V_2) < \mathscr{B}(B_F \to V_1(2S)V_2) < \mathscr{B}(B_F \to V_1(1S)V_2).$$

This is due to (i) the nodal structure of the participating daughter mesons in their excited states, (ii) tighter phase space and (iii) typical q^2-dependence of the weak decay form

Table 11 Decay widths in units of 10^{-15} GeV for general values of (a_1 and a_2) and branching fractions in % for three sets of Wilson coefficient a_1 and a_2

Decay modes	Decay width	Branching fraction			Experiment [87]
		a_1=1.12 $a_2 = -0.26$	a_1=1.14 $a_2 = -0.20$	a_1=0.93 $a_2 = -0.27$	
$\bar{B_s^0} \to D_s^{*+}(1S)D^{*-}$	$0.2714a_1^2$	0.0810	0.0839	0.0559	
$\bar{B_s^0} \to D_s^{*+}(2S)D^{*-}$	$0.0360a_1^2$	0.0107	0.0111	0.0074	
$\bar{B_s^0} \to D_s^{*+}(3S)D^{*-}$	$0.0117a_1^2$	0.0035	0.0036	0.0024	
$\bar{B^0} \to D^{*+}(1S)D^{*-}$	$0.3034a_1^2$	0.0878	0.0910	0.0605	
$\bar{B^0} \to D^{*+}(2S)D^{*-}$	$0.0359a_1^2$	0.0104	0.0107	0.0072	
$\bar{B^0} \to D^{*+}(3S)D^{*-}$	$0.0109a_1^2$	0.0032	0.0033	0.0022	
$\bar{B^0} \to D^{*+}(1S)D_s^{*-}$	$8.536a_1^2$	2.4712	2.5603	1.7039	0.8 ± 0.11
$\bar{B^0} \to D^{*+}(2S)D_s^{*-}$	$1.082a_1^2$	0.3133	0.3246	0.2160	
$\bar{B^0} \to D^{*+}(3S)D_s^{*-}$	$0.4534a_1^2$	0.1312	0.1359	0.0904	
$B^- \to D^{*0}(1S)D^{*-}$	$0.3043a_1^2$	0.0949	0.0984	0.0655	0.081 ± 0.017
$B^- \to D^{*0}(2S)D^{*-}$	$0.0357a_1^2$	0.0111	0.0115	0.0077	
$B^- \to D^{*0}(3S)D^{*-}$	$0.0102a_1^2$	0.0032	0.0033	0.0022	
$B^- \to D^{*0}(1S)D_s^{*-}$	$8.706a_1^2$	2.7180	2.8159	1.8740	1.71 ± 0.24
$B^- \to D^{*0}(2S)D_s^{*-}$	$1.0723a_1^2$	0.3347	0.3467	0.2307	
$B^- \to D^{*0}(3S)D_s^{*-}$	$0.7268a_1^2$	0.2268	0.2350	0.1564	

Table 12 Decay widths in units of 10^{-18} GeV for general values of (a_1 and a_2) and branching fractions in 10^{-6} for three sets of values of Wilson coefficient a_1 and a_2

Decay modes	Decay width	Branching fraction			[24]
		$a_1 = 1.12$ $a_2 = -0.26$	$a_1 = 1.14$ $a_2 = -0.20$	$a_1 = 0.93$ $a_2 = -0.27$	
$B_c^- \to D_s^{*-}(1S)D^{*0}$	$3.2453a_2^2$	0.1699	0.1005	0.1833	1.6
$B_c^- \to D_s^{*-}(2S)D^{*0}$	$0.7666a_2^2$	0.0401	0.0237	0.0433	
$B_c^- \to D_s^{*-}(3S)D^{*0}$	$0.1225a_2^2$	0.0064	0.0037	0.0069	
$B_c^- \to D^{*-}(1S)D^{*0}$	$0.0486a_2^2$	0.0025	0.0015	0.0027	21
$B_c^- \to D^{*-}(2S)D^{*0}$	$0.0224a_2^2$	0.0011	0.0006	0.0012	
$B_c^- \to D^{*-}(3S)D^{*0}$	$0.0036a_2^2$	0.0002	0.0001	0.0002	

Table 13 Decay widths in units of 10^{-15} GeV for general values of (a_1 and a_2) and branching fractions of order 10^{-6} for three sets of values of the Wilson coefficient a_1 and a_2

Decay mode	Decay width	Branching fraction		
		$a_1 = 1.12$ $a_2 = -0.26$	$a_1 = 1.14$ $a_2 = -0.20$	$a_1 = 0.93$ $a_2 = -0.27$
$B_c^- \to \bar{D}^{*0}(1S)D_s^{*-}$	$(0.0408a_1 + 0.0569a_2)^2$	0.741	0.956	0.395
$B_c^- \to \bar{D}^{*0}(1S)D^{*-}$	$(0.0069a_1 + 0.0069a_2)^2$	0.0279	0.0292	0.0164

factors for decay modes to higher excited ($2S$ and $3S$) states as compared to the decay to the ground ($1S$) states.

The relative size of branching fractions is broadly estimated from a power counting of QCD factors: (a_1, a_2) in the Wolfenstein parametrization. The class I decay modes characterized by a_1 are found to have large branching fractions, as expected; compared to those obtained for class II decays which are determined by a_2. The branching fractions of class III decays, characterized by Pauli interference for B_c-decays to two charmful states and obtained in $\mathcal{O}(10^{-6})$ can not be measured in current experiments.

Since the experimental data favor a constructive interference of the color-favored and color-suppressed b-flavored meson decays, the effect of Pauli interference is studied in dif-

Table 14 Predicted longitudinal fraction (R_L) and CP-odd fraction ($R_\perp$) in the b-flavored meson decays to two charmful vector meson states

Decay modes	Longitudinal polarization fraction(R_L)	CP-odd fraction($R_\perp$)
$B_c^- \to D_s^{*-}(1S)D^{*0}$	0.796	0.133
$B_c^- \to D_s^{*-}(2S)D^{*0}$	0.688	0.189
$B_c^- \to D_s^{*-}(3S)D^{*0}$	0.603	0.202
$B_c^- \to D^{*-}(1S)D^{*0}$	0.797	0.156
$B_c^- \to D^{*-}(2S)D^{*0}$	0.690	0.224
$B_c^- \to D^{*-}(3S)D^{*0}$	0.606	0.248
$B_c^- \to \bar{D}^{*0}(1S)D_s^{*-}$	0.725	0.138
$B_c^- \to \bar{D}^{*0}(1S)D^{*-}$	0.797	0.156
$\bar{B}_s^0 \to D_s^{*+}(1S)D^{*-}$	0.668	0.063
$\bar{B}_s^0 \to D_s^{*+}(2S)D^{*-}$	0.512	0.058
$\bar{B}_s^0 \to D_s^{*+}(3S)D^{*-}$	0.382	0.024
$\bar{B}^0 \to D^{*+}(1S)D^{*-}$	0.675	0.061
$\bar{B}^0 \to D^{*+}(2S)D^{*-}$	0.514	0.057
$\bar{B}^0 \to D^{*+}(3S)D^{*-}$	0.381	0.023
$\bar{B}^0 \to D^{*+}(1S)D_s^{*-}$	0.646	0.063
$\bar{B}^0 \to D^{*+}(2S)D_s^{*-}$	0.482	0.054
$\bar{B}^0 \to D^{*+}(3S)D_s^{*-}$	0.350	0.009
$B^- \to D^{*0}(1S)D^{*-}$	0.675	0.061
$B^- \to D^{*0}(2S)D^{*-}$	0.502	0.055
$B^- \to D^{*0}(3S)D^{*-}$	0.390	0.026
$B^- \to D^{*0}(1S)D_s^{*-}$	0.647	0.063
$B^- \to D^{*0}(2S)D_s^{*-}$	0.470	0.051
$B^- \to D^{*0}(3S)D_s^{*-}$	0.358	0.014

ferent decay modes, by evaluating an enhancement factor in the decay mode. For $B_c^- \to J/\psi D_s^{*-}$, $B_c^- \to \psi(2S)D_s^{*-}$, $B_c^- \to J/\psi D^{*-}$ and $B_c^- \to \psi(2S)D^{*-}$, the enhancement factor (in %) are found to be $\sim$ 56, $\sim$ 97, $\sim$ 33, and $\sim$ 99, respectively, where as for $B_c^- \to \bar{D}^{*0}D_s^{*-}$ and $B_c^- \to \bar{D}^{*0}D^{*-}$, it is found to be $\sim$ 4 and $\sim$ 3, respectively. This shows that the Pauli interference is less significant in B_c^--decays to two charmful states: $B_c^- \to \bar{D}^{*0}D_{(s)}^{*-}$ compared to its other decay modes. However, study of these modes is important as they have been proposed for extracting the CKM angle γ through amplitude relation.

The longitudinal polarization fraction (R_L) and CP-odd fraction ($R_\perp$) are predicted for all decay modes considered the present analysis, where R_Ls dominate over $R_\perp$s as shown in Tables 14, 15. The CP-odd fraction in nonleptonic B_c^--decays to two charmful states are obtained one order magnitude higher than that in other b-flavored meson decays. For color-favored $B_c^- \to D^* D_{(s)}^{*-}$ decay, the effect arising due to the short-distance non-spectator contribution is shown to be marginal. However, the long-distance (LD) nonfactorizable contributions from rescattering effects, final-state interactions, etc., may not be negligible. If a significant LD effect exists, one expects large CP-odd fractions in these decay modes. Our predicted $R_\perp$ for $B \to D^* D_{(s)}^*$ decay modes, in particular, are found slightly smaller than other model pre-

Table 15 Predicted longitudinal fraction (R_L) and CP-odd fraction ($R_\perp$) in B_c^-, B^-, $\bar{B}^0$, $\bar{B}_s^0$ decays to charmonium and charm meson states

Decay modes	Longitudinal polarization fraction(R_L)	CP-odd fraction($R_\perp$)
$B_c^- \to J/\psi\rho^-$	0.932	0.018
$B_c^- \to \psi(2S)\rho^-$	0.891	0.024
$B_c^- \to \psi(3S)\rho^-$	0.853	0.026
$B_c^- \to J/\psi K^{*-}$	0.911	0.023
$B_c^- \to \psi(2S)K^{*-}$	0.860	0.030
$B_c^- \to \psi(3S)K^{*-}$	0.813	0.032
$B_c^- \to J/\psi D_s^{*-}$	0.570	0.185
$B_c^- \to \psi(2S)D_s^{*-}$	0.479	0.296
$B_c^- \to \psi(3S)D_s^{*-}$	0.343	0.302
$B_c^- \to J/\psi D^{*-}$	0.585	0.217
$B_c^- \to \psi(2S)D^{*-}$	0.482	0.378
$B_c^- \to \psi(3S)D^{*-}$	0.443	0.402
$B^- \to \rho^- J/\psi$	0.750	0.149
$B^- \to \rho^-\psi(2S)$	0.542	0.265
$B^- \to \rho^-\psi(3S)$	0.420	0.341
$B^- \to K^{*-}J/\psi$	0.721	0.152
$B^- \to K^{*-}\psi(2S)$	0.547	0.189
$B^- \to K^{*-}\psi(3S)$	0.415	0.200
$B^- \to D^{*0}(1S)\rho^-$	0.945	0.013
$B^- \to D^{*0}(2S)\rho^-$	0.895	0.021
$B^- \to D^{*0}(3S)\rho^-$	0.849	0.024
$B^- \to D^{*0}(1S)K^{*-}$	0.928	0.017
$B^- \to D^{*0}(2S)K^{*-}$	0.865	0.027
$B^- \to D^{*0}(3S)K^{*-}$	0.807	0.030
$\bar{B}^0 \to D^{*+}(1S)\rho^-$	0.945	0.013
$\bar{B}^0 \to D^{*+}(2S)\rho^-$	0.899	0.020
$\bar{B}^0 \to D^{*+}(3S)\rho^-$	0.845	0.025
$\bar{B}^0 \to D^{*+}(1S)K^{*-}$	0.928	0.017
$\bar{B}^0 \to D^{*+}(2S)K^{*-}$	0.870	0.026
$\bar{B}^0 \to D^{*+}(3S)K^{*-}$	0.802	0.031
$\bar{B}_s^0 \to D_s^{+*}(1S)\rho^-$	0.943	0.014
$\bar{B}_s^0 \to D_s^{+*}(2S)\rho^-$	0.898	0.021
$\bar{B}_s^0 \to D_s^{+*}(3S)\rho^-$	0.845	0.025
$\bar{B}_s^0 \to D_s^{+*}(1S)K^{*-}$	0.925	0.018
$\bar{B}_s^0 \to D_s^{+*}(2S)K^{*-}$	0.868	0.027
$\bar{B}_s^0 \to D_s^{+*}(3S)K^{*-}$	0.803	0.031

dictions. This is due to large helicity amplitude $\mathscr{A}_{ll}$ and small value of the form factor $g(q^2)$ obtained in our model.

In conclusion, the present analysis shows that the factorization approximation works reasonably well in describing the exclusive nonleptonic $B_F \to V_1(nS)V_2$ decays in the framework of the RIQ model.

Acknowledgements The library and computational facilities provided by authorities of Siksha 'O' Anusandhan Deemed to be University, Bhubaneswar, 751030, India are duly acknowledged.

Data Availability Statement This manuscript has no associated data or the data will not be deposited. [Authors' comment: In the present study, while predicting the decay processes in the context of our relativistic independent quark (RIQ) model, we have only used the existing experimental data from Particle Data Group along with our model parameters which have been fixed from hadron spectroscopy. As such there is no freedom left in our calculation. Hence, there is no data that can be deposited.]

Funded by SCOAP[3]. SCOAP[3] supports the goals of the International Year of Basic Sciences for Sustainable Development.

Appendix A: Quark orbitals and wave packet representation of the meson state in RIQ model framework

In the RIQ model, a meson is picturized as a color-singlet assembly of a quark and an antiquark independently confined by an effective and average flavor-independent potential in the form: $U(r) = \frac{1}{2}(1+\gamma^0)(ar^2+V_0)$, where (a, V_0) are the potential parameters. It is believed that the zeroth-order quark dynamics generated by the phenomenological confining potential $U(r)$ taken in equally mixed scalar-vector harmonic form can provide an adequate tree-level description of the decay process being analyzed in this work. With the interaction potential $U(r)$ put into the zeroth-order quark lagrangian density, the ensuing Dirac equation admits a static solution of positive and negative energy as:

$$\begin{aligned}\psi_\xi^{(+)}(\mathbf{r}) &= \begin{pmatrix} \frac{ig_\xi(r)}{r} \\ \frac{\boldsymbol{\sigma}.\hat{r} f_\xi(r)}{r} \end{pmatrix} \chi_{l,j,m_j}(\hat{r}),\\ \psi_\xi^{(-)}(\mathbf{r}) &= \begin{pmatrix} \frac{i(\boldsymbol{\sigma}.\hat{r}) f_\xi(r)}{r} \\ \frac{g_\xi(r)}{r} \end{pmatrix} \tilde{\chi}_{l,j,m_j}(\hat{r}), \end{aligned} \tag{A.1}$$

where, $\xi = (nlj)$ represents a set of Dirac quantum numbers specifying the eigenmodes. $\chi_{ljm_j}(\hat{r})$ and $\tilde{\chi}_{ljm_j}(\hat{r})$ are the spin angular parts given by,

$$\begin{aligned}\chi_{ljm_j}(\hat{r}) &= \sum_{m_l,m_s} < lm_l \ \frac{1}{2} m_s | jm_j > Y_l^{m_l}(\hat{r}) \chi_{\frac{1}{2}}^{m_s},\\ \tilde{\chi}_{ljm_j}(\hat{r}) &= (-1)^{j+m_j-l} \chi_{lj-m_j}(\hat{r}). \end{aligned} \tag{A.2}$$

With the quark binding energy parameter E_q and quark mass parameter m_q written in the form $E_q' = (E_q - V_0/2)$, $m_q' = (m_q + V_0/2)$ and $\omega_q = E_q' + m_q'$, one can obtain solutions to the resulting radial equation for $g_\xi(r)$ and $f_\xi(r)$ in the form:

$$\begin{aligned} g_{nl} &= N_{nl}\Big(\frac{r}{r_{nl}}\Big)^{l+1} \exp(-r^2/2r_{nl}^2) L_{n-1}^{l+1/2}(r^2/r_{nl}^2),\\ f_{nl} &= \frac{N_{nl}}{r_{nl}\omega_q}\Big(\frac{r}{r_{nl}}\Big)^{l} \exp(-r^2/2r_{nl}^2)\\ &\quad \times \Big[\Big(n+l-\frac{1}{2}\Big) L_{n-1}^{l-1/2}(r^2/r_{nl}^2) + n L_n^{l-1/2}(r^2/r_{nl}^2)\Big], \end{aligned} \tag{A.3}$$

where, $r_{nl} = (a\omega_q)^{-1/4}$ is a state independent length parameter, N_{nl} is an overall normalization constant given by

$$N_{nl}^2 = \frac{4\Gamma(n)}{\Gamma(n+l+1/2)} \frac{(\omega_{nl}/r_{nl})}{(3E_q' + m_q')}, \tag{A.4}$$

and $L_{n-1}^{l+1/2}(r^2/r_{nl}^2)$ etc. are associated Laguerre polynomials. The radial solutions yield an independent quark bound-state condition in the form of a cubic equation:

$$\sqrt{(\omega_q/a)}(E_q' - m_q') = (4n + 2l - 1). \tag{A.5}$$

From the solution of the cubic equation (A.5), the zeroth-order binding energies of the confined quark and antiquark are obtained for all possible eigenmodes.

In the relativistic independent particle picture of this model, the relativistic constituent quark and antiquark are thought to move independently inside the meson bound-state $|B_F(\mathbf{p}, S_{B_F})\rangle$ with their momentum $\mathbf{p}_b$ and $\mathbf{p}_{\bar{q}}$, respectively. In order to study the decay process which takes place in the momentum eigenstates of participating mesons, we Fourier transform the quark orbitals (A.1) to momentum space and obtain the momentum probability amplitude of the quark and antiquark of participating mesons in the following forms: For ground state mesons: $(n = 1, l = 0)$,

$$\begin{aligned} G_b(\mathbf{p}_b) &= \frac{i\pi\mathscr{N}_b}{2\alpha_b\omega_b}\sqrt{\frac{(E_{p_b}+m_b)}{E_{p_b}}}(E_{p_b}+E_b)\\ &\quad \times \exp\Big(-\frac{\mathbf{p_b}^2}{4\alpha_b}\Big),\\ \tilde{G}_{\bar{q}}(\mathbf{p}_{\bar{q}}) &= -\frac{i\pi\mathscr{N}_{\bar{q}}}{2\alpha_{\bar{q}}\omega_{\bar{q}}}\sqrt{\frac{(E_{p_{\bar{q}}}+m_{\bar{q}})}{E_{p_{\bar{q}}}}}(E_{p_{\bar{q}}}+E_{\bar{q}}) \end{aligned}$$

$$\times \exp\Big(-\frac{\mathbf{p}_{\bar{q}}^2}{4\alpha_{\bar{q}}}\Big). \tag{A.6}$$

For the excited meson state: $(n=2, l=0)$,

$$\begin{aligned} G_b(\mathbf{p}_b) &= \frac{i\pi\mathscr{N}_b}{2\alpha_b\omega_b}\sqrt{\frac{(E_{p_b}+m_b)}{E_{p_b}}}(E_{p_b}+E_b) \\ &\quad\times\Big(\frac{\mathbf{p_b}^2}{2\alpha_b}-\frac{3}{2}\Big)\exp\Big(-\frac{\mathbf{p_b}^2}{4\alpha_b}\Big), \\ \tilde{G}_{\bar{q}}(\mathbf{p}_{\bar{q}}) &= -\frac{i\pi\mathscr{N}_{\bar{q}}}{2\alpha_{\bar{q}}\omega_{\bar{q}}}\sqrt{\frac{(E_{p_{\bar{q}}}+m_{\bar{q}})}{E_{p_{\bar{q}}}}}(E_{p_{\bar{q}}}+E_{\bar{q}}) \\ &\quad\times\Big(\frac{\mathbf{p}_{\bar{q}}^2}{2\alpha_{\bar{q}}}-\frac{3}{2}\Big)\exp\Big(-\frac{\mathbf{p}_{\bar{q}}^2}{4\alpha_{\bar{q}}}\Big). \end{aligned} \tag{A.7}$$

For the excited meson state: $(n=3, l=0)$,

$$\begin{aligned} G_b(\mathbf{p}_b) &= \frac{i\pi\mathscr{N}_b}{2\alpha_b\omega_b}\sqrt{\frac{(E_{p_b}+m_b)}{E_{p_b}}}(E_{p_b}+E_b) \\ &\quad\times\Big(\frac{\mathbf{p}_b{}^4}{8\alpha_b^2}-\frac{5\mathbf{p_b}^2}{4\alpha_b}+\frac{15}{8}\Big)\exp\Big(-\frac{\mathbf{p_b}^2}{4\alpha_b}\Big), \\ \tilde{G}_{\bar{q}}(\mathbf{p}_{\bar{q}}) &= -\frac{i\pi\mathscr{N}_{\bar{q}}}{2\alpha_{\bar{q}}\omega_{\bar{q}}}\sqrt{\frac{(E_{p_{\bar{q}}}+m_{\bar{q}})}{E_{p_{\bar{q}}}}}(E_{p_{\bar{q}}}+E_{\bar{q}}) \\ &\quad\times\Big(\frac{\mathbf{p}_{\bar{q}}{}^4}{8\alpha_{\bar{q}}^2}-\frac{5\mathbf{p}_{\bar{q}}^2}{4\alpha_{\bar{q}}}+\frac{15}{8}\Big)\exp\big(-\frac{\mathbf{p}_{\bar{q}}^2}{4\alpha_{\bar{q}}}\big). \end{aligned} \tag{A.8}$$

With the momentum probability amplitudes of quark constituents, we construct an effective momentum distribution function for the meson state in the form $\mathscr{G}_{B_F}(\mathbf{p}_b,\ \mathbf{p}_{\bar{q}}) = \sqrt{G_b(\mathbf{p}_b)G_{\bar{q}}(\mathbf{p}_{\bar{q}})}$ in the light of an ansatz of Margolis and Mendel in their bag model description of the meson bound state [104].

Here the effective momentum distribution function $\mathscr{G}_{B_F}(\mathbf{p}_b, \mathbf{p}_{\bar{q}})$, which in fact, embodies the bound-state characteristics of $|B_F(\mathbf{p}, S_{B_F})\rangle$, defines the meson bound state at definite momentum $\mathbf{p}$ and spin projection S_{B_F} in the form:

$$\begin{aligned} |B_F(\mathbf{p}, S_{B_F})\rangle &= \hat{\Lambda}(\mathbf{p}, S_{B_F})|(\mathbf{p}_b,\lambda_b);(\mathbf{p}_{\bar{q}},\lambda_{\bar{q}})\rangle \\ &= \hat{\Lambda}(\mathbf{p}, S_{B_F})\hat{b}_b^{\dagger}(\mathbf{p}_b,\lambda_b)\hat{\bar{b}}_{\bar{q}}^{\dagger}(\mathbf{p}_{\bar{q}},\lambda_{\bar{q}})|0\rangle, \end{aligned} \tag{A.9}$$

where $|(\mathbf{p}_b,\lambda_b);(\mathbf{p}_{\bar{q}},\lambda_{\bar{q}})\rangle$ is the Fock-space representation of unbound quark and antiquark in a color-singlet configuration with respective momentum and spin: $(\mathbf{p}_b,\lambda_b)$ and $(\mathbf{p}_{\bar{q}},\lambda_{\bar{q}})$. $\hat{b}_b^{\dagger}(\mathbf{p}_b,\lambda_b)$ and $\hat{\bar{b}}_{\bar{q}}^{\dagger}(\mathbf{p}_{\bar{q}},\lambda_{\bar{q}})$ are the quark and antiquark creation operators and $\hat{\Lambda}(\mathbf{p}, S_{B_F})$ is a bag-like integral operator taken in the form:

$$\begin{aligned} \hat{\Lambda}(\mathbf{p}, S_{B_F}) &= \frac{\sqrt{3}}{\sqrt{N_{B_F}(\mathbf{p})}}\sum_{\lambda_b,\lambda_{\bar{q}}}\zeta_{b,\bar{q}}^{B_F}\int d^3\mathbf{p}_b\, d^3\mathbf{p}_{\bar{q}} \\ &\quad\times\delta^{(3)}(\mathbf{p}_b+\mathbf{p}_{\bar{q}}-\mathbf{p})\,\mathscr{G}_{B_F}(\mathbf{p}_b,\mathbf{p}_{\bar{q}}). \end{aligned} \tag{A.10}$$

Here, $\sqrt{3}$ is the effective color factor and $\zeta_{b,\bar{q}}^{B_F}$ is the $SU(6)$ spin-flavor coefficients for the B_F-meson state. Imposing the normalization condition in the form $\langle B_F(\mathbf{p})|B_F(\mathbf{p}')\rangle = \delta^{(3)}(\mathbf{p}-\mathbf{p}')$, the meson state normalization $N_{B_F}(\mathbf{p})$ is obtainable in an integral form

$$N_{B_F}(\mathbf{p}) = \int d^3\mathbf{p}_b\,|\mathscr{G}_{B_F}(\mathbf{p}_b,\ \mathbf{p}_{\bar{q}})|^2. \tag{A.11}$$

References

1. G.S. Abrams et al., Phys. Rev. Lett. **33**, 1453 (1974)
2. S.-K. Choi et al., Phys. Rev. Lett. **89**, 102001 (2002)
3. BELLE collaboration, Observation of a new $D_{(sJ)}$ meson in $B^+ \to \bar{D}^0 D^0 K^+$ decays. Phys. Rev. Lett. **100**, 092001 (2008). arXiv:0707.3491
4. T. Matsuki, T. Morii, K. Sudho, Radial excitation of heavy mesons. Eur. Phys. J. A **31**, 701 (2007). arXiv:hep-ph/0610186
5. LHCb collaboration, Determination of quantum numbers for several excited charmed mesons observed in $B^- \to D^{*+}\pi^-\pi^-$ decays. Phys. Rev. D **101**, 032005 (2020). arXiv:1911.05957
6. S. Godfrey, N. Isgur, Mesons in a relativized quark model with chromodynamics. Phys. Rev. D **32**, 189 (1985)
7. LHCb collaboration, Study of D_J meson decays to $D^+\pi^-$, $D^0\pi^+$ and $D^{*+}\pi^-$ final states in pp collision. JHEP **09**, 145 (2013). arXiv:1307.4556
8. DELPHI collaboration, First evidence for a charm radially excitation, $D^{*'}$. Phys. Lett. B **426**, 231 (1998)
9. LHCb collaboration, Amplitude analysis of $B^- \to D^+\pi^-\pi^-$ decays. Phys. Rev. D **94**, 072001 (2016). arXiv:1608.01289
10. BELLE collaboration, Measurement of branching fraction ratios and CP asymmetries in $B^\pm \to D_{CP}K^\pm$. Phys. Rev. D **68**, 051101 (2003). arXiv:hep-ex/0304032
11. BABAR collaboration, Branching fraction measurement of $\bar{B}^0 \to D^{(*)+}\pi^-$ and $B^- \to D^{(*)0}\pi^-$ and isospin analysis of $\bar{B} \to D^{(*)}\pi$ decays. Phys. Rev. D **75**, 031101 (2007). arXiv:hep-ex/0610027
12. LHCb collaboration, Measurement of branching fraction of decays $B_s^0 \to D_s^{\mp}K^{\pm}$ and $B_s^0 \to D_s^-\pi^+$. JHEP **06**, 115 (2012). arXiv:1204.1237
13. R. Aaij et al. [LHCb collaboration], Phys. Rev. D **87**(11), 112012 (2013). Addendum: [Phys. Rev. D **89**(1), 019901 (2014)] .arXiv:1304.4530 [hep-ex]
14. G. Aad et al. [ATLAS Collaboration], Eur. Phys. J. C **76**(1), 4 (2016). arXiv:1507.07099 [hep-ex]
15. X. Liu, Z-J. Xiao, C-D. Lu, Phys. Rev. D **81**, 014022 (2010)
16. C.-H. Chang, Y.-Q. Chen, The decays of $B_{(c)}$ meson. Phys. Rev. D **49**, 3399 (1994)
17. C. Chang, H.-F. Fu, G.-L. Wang, J.-M. Zhang, Some of semileptonic and nonleptonic decays of B_c meson in a Bethe-Salpeter relativistic quark model. Sci. China Phys. Mech. Astron. **58**, 071001 (2015). (**[1411.3428]**)
18. J.-F. Liu, K.-T. Chao, B_c meson weak decays and CP-violation. Phys. Rev. D **56**, 4133 (1997)
19. T. Zhou et al., J. Phys. G Nucl. Part. Phys. **48**, 055006 (2021)
20. T. Zhou et al., Eur. Phys. J. C **81**, 339 (2021)
21. D. Ebert, R.N. Faustov, V.O. Galkin, Phys. Rev. D **68**, 094020 (2003)
22. M.A. Ivanov, J.G. Korner, P. Santorelli, Phys. Rev. D **71**, 094020 (2005)
23. M.A. Ivanov, J.G. Korner, P. Santorelli, Phys. Rev. D **63**, 074010 (2001)

24. M.A. Ivanov, J.G. Korner, P. Santorelli, Phys. Rev. D **73**, 054024 (2006)
25. I. Bediaga, J. H. Munoz, Production of radially excited charmonium mesons in two-body nonleptonic B_c decays (2011). arXiv:1102.2190
26. H.-W. Ke, T. Liu, X.-Q. Li, Phys. Rev. D **89**, 017501 (2014)
27. R.N. Faustov, V.O. Galkin, Phys. Rev. D **87**, 034033 (2013)
28. P. Colangelo, F. De Fazio, Phys. Rev. D **61**, 034012 (2000)
29. M. Beneke, G. Buchalla, M. Neubert, C.T. Sachrajda, QCD factorization for exclusive, nonleptonic B meson decays: general arguments and the case of heavy light final states. Nucl. Phys. B **591**, 313 (2000). arXiv:hep-ph/0006124
30. R.-H. Li, C.-D. Lu, H. Zou, The $B(B_{(s)}) \to D_{(s)}P$, $D_{(s)}V$, $D^*_{(s)}P$ and $D^*_{(s)}V$ decays in the perturbative QCD approach. Phys. Rev. D **78**, 014018 (2008). arXiv:0803.1073
31. G. Li, F.l. Shao,W. Wang, $B_s \to D_s(3040)$ form factors and B_s decays into $D_s(3040)$. Phys. Rev. D **82**, 094031 (2010). arXiv:1008.3696
32. R.-H. Li, C.-D. Lu, Y.-M. Wang, Exclusive B_s decays to the charmed mesons $D_s^+(1968, 2317)$ in the standard model. Phys. Rev. D **80**, 014005 (2009). arXiv:0905.3259
33. M. Neubert, B. Stech, Nonleptonic weak decays of B mesons, arXiv:hep-ph/9705292
34. N. Barik, P.C. Dash, Phys. Rev. D **63**, 114002 (2001)
35. S. Naimuddin, S. Kar, M. Priyadarshini, N. Barik, P.C. Dash, Phys. Rev. D **86**, 094028 (2012)
36. N. Barik, S. Naimuddin, P.C. Dash, S. Kar, Phys. Rev. D **80**, 014004 (2009)
37. S. Kar, P.C. Dash, M. Priyadarsini, S. Naimuddin, N. Barik, Phys. Rev. D **88**, 094014 (2013)
38. M. Wirbel, B. Stech, M. Bauer, Z. Phys. C **29**, 637 (1985)
39. M. Bauer, B. Stech, M. Wirbel, Z. Phys. C **103**, 34 (1987)
40. L.-L. Chau, H.-Y. Cheng, W.K. Sze, H. Yao, B. Tseng, Phys. Rev. D **43**, 2176 (1991)
41. L.-L. Chau, H.-Y. Cheng, W.K. Sze, H. Yao, B. Tseng, Phys. Rev. D **58**, 019902 (1998)
42. I.P. Gouz, V.V. Kiselev, A.K. Likhoded, V.I. Romanovsky, O.P. Yushchenko, Phys. At. Nucl. **67**, 1559 (2004)
43. M. Beneka, G. Buchalla, M. Neubert, C.T. sachrajda, Phys. Rev. Lett. **83**, 1914 (1999)
44. M. Beneka, G. Buchalla, M. Neubert, C.T. Sachrajda, Nucl. Phys. B **591**, 313 (2000)
45. M. Beneka, G. Buchalla, M. Neubert, C.T. Sachrajda, Nucl. Phys. B **606**, 245 (2001)
46. M. Beneka, M. Neubert, Nucl. Phys. B **675**, 33 (2003)
47. C.E. Thomas, Phys. Rev. D **73**, 054016 (2006)
48. V.V. Kiselev, A.E. Kovalsky, A.K. Likhoded, Phys. At. Nucl. **64**, 1860 (2001)
49. V.V. Kiselev, A.E. Kovalsky, A.K. Likhoded, Nucl. Phys. B **585**, 353 (2000)
50. V.V. Kiselev, (2002). arXiv: hep-ph/0211021
51. X.Q. Yu, X.L. Zhou, Phys. Rev. D **81**, 037501 (2010)
52. J.D. Bjorken, in Proceedings of the International Workshop, Crete, Greece, 1988, edited by G. Branco and J. Reeo, Development in High Energy Physics, Nucl. Phys. B Proc. Suppl. **11** , 325 (1989)
53. A.J. Buras, J.M. Gerard, R. Ruckl, Nucl. Phys. B **268**, 16 (1986)
54. M. Neubert, Phys. Rep. **245**, 259 (1994)
55. G. Buchalla et al., Eur. Phys. J. C **57**, 309 (2008). A.J. Buras, arXiv:hep-ph/9806471
56. L. Nayak, P.C. Dash, S. Kar, N. Barik, Phys. Rev. D **105**, 053007 (2022)
57. R. Aajj et al. (LHCb Collaboration), J. High Energy Phys. **09**, 075 (2013)
58. N. Brambilla et al. (Quarkonium Working Group), arXiv:hep-ph/0412158
59. M. Neubert, B. Stech, Adv. Ser. Dir. High Energy Phys. **17**, 294 (1998)
60. H.M. Choi, C.R. Ji, Phys. Rev. D **80**, 114003 (2009)
61. J. Sun, D. Du, Y. Yang, Eur. Phys. J. C **60**, 107 (2009)
62. J. Sun, Y. Yang, W. Du, H. Ma, Phys. Rev. D **77**, 114004 (2008)
63. J. Sun, G. Xue, Y. Yang, G. Lu, D. Du, Phys. Rev. D **77**, 074013 (2008)
64. P. Colangelo, F. De Fazio, Phys. Rev. D **61**, 034012 (2000)
65. N. Sharma, R.C. Verma, Phys. Rev. D **82**, 094014 (2010)
66. N. Sharma, R. Dhir, R.C. Verma, J. Phys. G **37**, 075013 (2010)
67. R. Dhir, R.C. Verm, Phys. Rev. D **79**, 034004 (2009)
68. N. Sharma, Phys. Rev. D **81**, 014027 (2010)
69. N. Barik, S. Naimuddin, P.C. Dash, S. Kar, Phys. Rev. D **77**, 014038 (2008)
70. N. Barik, S. Naimuddin, P.C. Dash, S. Kar, Phys. Rev. D **78**, 114030 (2008)
71. N. Barik, S. Naimuddin, P.C. Dash, Int. J. Mod. Phys. A **24**, 2335 (2009)
72. P. Colangelo, F. De Fazio, G. Nardulli, Phys. Lett. B **386**, 328 (1996)
73. G. Altarelli, N. Cabibbo, G. Corbo, L. Maiani, G. Martinelli, Nucl. Phys. B **208**, 365 (1982)
74. N. Barik, B.K. Dash, Phys. Rev. D **33**, 1925 (1986)
75. N. Barik, B.K. Dash, P.C. Dash, Pramana J. Phys. **29**, 543 (1987)
76. N. Barik, P.C. Dash, Phys. Rev. D **47**, 2788 (1993)
77. N. Barik, P.C. Dash, A.R. Panda, Phys. Rev. D **46**, 3856 (1992)
78. N. Barik, P.C. Dash, Mod. Phys. Lett. A **10**, 103 (1995)
79. N. Barik, S. Kar, P.C. Dash, Phys. Rev. D **57**, 405 (1998)
80. N. Barik, P.C. Dash, A.R. Panda, Phys. Rev. D **47**, 1001 (1994)
81. N. Barik, P.C. Dash, Phys. Rev. D **53**, 1336 (1996)
82. N. Barik, S.K. Tripathy, S. Kar, P.C. Dash, Phys. Rev. D **56**, 4238 (1997)
83. N. Barik, S. Naimuddin, P.C. Dash, S. Kar, Phys. Rev. D **80**, 074005 (2009)
84. S. Patnaik, L. Nayak, P.C. Dash, S. Kar, N. Barik, Eur. Phys. J. Plus. **135**, 1336 (2020)
85. L. Nayak, S. Patnaik, P.C. Dash, S. Kar, N. Barik, Phys. Rev. D **104**, 036012 (2021)
86. L. Nayak, P.C. Dash, S. Kar, N. Barik, Eur. Phys. J. C **82**, 750 (2022)
87. R.L. Workman et al. (Particle Data Group), Prog. Theor. Exp. Phys. **2022**, 283C01 (2022)
88. P.A. Zyla et al. (Particle Data Group), Prog. Theor. Exp. Phys. **2020**, 083C01 (2020)
89. S. Godfrey, K. Moats, Phys. Rev. D **93**, 034035 (2016)
90. T.E. Browder, K. Honscheid, Prog. Part. Nucl. Phys. **35**, 81 (1995)
91. M. Neubert, V. Rieckert, B. Stech, Q.P. Xu, in Heavy Flavors, edited by A.J. Buras, H. Lindner (World Scientific, Singapore, 1992) and references therein
92. S. Dubnika, A.Z. Dubnikov, A. Issadykov, M.A. Ivanov, A. Liptaj, Phys. Rev. D **96**, 076017 (2017)
93. Y.-Y. Fan, Z.-J. Xiao, R.-M. Wang, B.-Z. Li, Sci. Bull. **60**(23), 2009–2015 (2015)
94. J. Harrison, C.T.H. Davies, A. Lytle (HPQCD Collaboration), Phys. Rev. D **102**, 094518 (2020)
95. G.-L. Wang, X.-G. Wu, Chin. Phys. C **44**, 063104 (2020)
96. L. Wolfenstein, Phys. Rev. Lett. **51**, 1945 (1983)
97. V.V. Kiselev, J. Phys. G **30**, 1445 (2004)
98. R. Fleischer, D. Wyler, Phys. Rev. D **62**, 057503 (2000)
99. M. Masetti, Phys. Lett. B **286**, 160 (1992)
100. M.A. Ivanov, J.G. Korner, O.N. Pakhomova, Phys. Lett. B **555**, 189 (2003)
101. H.N. Li, S. Mishima, Phys. Rev. D **71**, 054025 (2005)
102. D. Melikhov, B. Stech, Phys. Rev. D **62**, 014006 (2000)
103. H.Y. Cheng, C.K. Chua, C.W. Hwang, Phys. Rev. D **69**, 074025 (2004)
104. B. Margolis, R.R. Mendel, Phys. Rev. D **28**, 468 (1983)